

Eco-evolutionary dynamics of infection and immunity in experimentally founded lake populations of threespine stickleback

Daniel I. Bolnick,^{1*} Lucas Eckert,² Rowan D.H. Barrett,² Emma Choi,¹ Grant Haines,^{2,3}
Andrew P. Hendry,² Emily V. Kerns,⁴ Åsa J. Lind,^{2,5} Kathryn Milligan-McClellan,⁶
Catherine L. Peichel,⁵ Kristofer Sasser,⁴ Alice R Thornton,⁷ Cole Wolf,⁴ Natalie C.
Steinel,^{7,8} Jesse N. Weber^{4*}

¹ Department of Ecology and Evolutionary Biology, University of Connecticut Storrs CT, USA.

² Department of Biology, McGill University, Montreal, Quebec, Canada

³ University of Holar, Holar, Iceland

⁴ Department of Integrative Biology, University of Wisconsin, Madison, WI, USA

⁵ Division of Evolutionary Ecology, Institute of Ecology and Evolution, University of Bern, Bern, Switzerland

⁶ Department of Molecular and Cell Biology, University of Connecticut, Storrs, CT, USA

⁷ Center for Pathogen Research and Training, University of Massachusetts, Lowell, MA, USA

⁸ Department of Biology, University of Massachusetts, Lowell, USA

*Corresponding authors. Email: daniel.bolnick@uconn.edu or jnweber2@wisc.edu

MS type: Article

ORCID IDs:

Bolnick: 0000-0003-3148-6296

Eckert: 0000-0003-3718-773X

Barrett: 0000-0003-3044-2531

Choi:0000-0003-2799-3914

Haines: 0000-0007-9085-0022

Hendry: 0000-0002-4807-6667

Kerns: 0009-0002-0538-4632

Lind: 0000-0003-2553-567X

Milligan-McClellan: 0000-0002-8479-0809

Peichel: 0000-0002-7731-8944

Sasser: 0000-0002-0449-0815

Thornton: 0009-0004-8927-2842

Wolf: 0000-0001-5354-9169

Steinel: 0000-0002-7585-8402

Weber: 0000-003-4839-6684

Abstract:

Host-parasite interactions are likely to involve eco-evolutionary feedbacks. Parasites can impose strong selection on host immune traits. Evolution of these traits can suppress parasite abundance, which alters the strength of selection. Such eco-evo feedbacks can be hard to document in natural settings, where long-term interactions may have converged on relatively stable equilibria. However, when a species disperses into an unoccupied habitat, it can experience altered parasite abundance (e.g., enemy release), or encounter new parasite genotypes. These perturbations may be followed by observable eco-evolutionary dynamics as the newly assembled host-parasite communities interact and evolve. To test this hypothesis, we experimentally founded nine whole-lake populations of threespine stickleback, and tracked changes in the prevalence of a parasite (*Schistocephalus solidus*) and a heritable host immune trait (fibrosis) for seven years. In native source lakes, among-population differences in tapeworm prevalence and fibrosis were relatively stable across years, suggesting there are alternative eco-evolutionary equilibria. In contrast, the experimentally founded populations initially exhibited enemy release, followed by strong year-to-year fluctuations in infection and fibrosis. In lakes with high initial infection rates, fibrosis subsequently increased in severity, suppressing infections. Conversely, low fibrosis was followed by increased parasite prevalence. This temporal autocorrelation between parasite prevalence and immune traits weakened over time. These results are consistent with the existence of transient eco-evolutionary dynamics between host and parasite in newly founded populations.

Key words: Experimental Evolution, Eco-immunology, Ecological Release,

Gasterosteus aculeatus, *Schistocephalus solidus*

INTRODUCTION

Host-parasite interactions are expected to be an important source of eco-evolutionary dynamics. Parasites can impose especially strong selection on hosts (Fumagalli et al. 2011; Seppälä 2015). The resulting rapid evolution of immune genes and traits should drive ecological changes in parasite abundance (e.g., Feis et al 2016). Evolution of greater resistance can suppress infections, whereas tolerance can increase parasite prevalence (Koskella 2018). These ecological changes can then feed-back to modify the strength of selection acting on immune traits.

These eco-evo dynamics are hard to detect in nature (Pelletier et al. 2007, 2009; Hendry 2017). Studies must document coupled changes in parasite prevalence and heritable changes in the relevant host immune traits, spanning multiple generations. When such long-term datasets exist, they often rely on single instances of biological invasions, or follow single populations. This lack of replication makes it harder to rule out alternative explanations such as mutual dependence on unmeasured environmental fluctuations. To further complicate matters, eco-evo dynamics may be transient, weakening and becoming undetectable as populations converge on a stable equilibrium combination of parasite abundance and host immune traits.

One solution can be to study eco-evo dynamics in perturbed communities. Species frequently disperse into unoccupied habitats, founding new populations or driving range expansion (Hanski 1998; Parmesan et al. 1999; Walsh et al. 2016). New host populations can experience reduced infection (‘enemy release’; Torchin et al. 2003; Liu and Stiling 2006; Trewby et al. 2007; Schatz and Park 2023), or gain new parasites (Kelly et al. 2009; Marzal et al. 2011; Shaw et al. 2024; Sriramulu et al. 2025). Eco-evolutionary models indicate that these new populations can experience cycles of increasing infection, then increased immunity, then reduced infection, ending in a new equilibrium state (Fleisher et al. 2021; Wilber et al. 2024; Cortez et al. 2024.; Kilsdonk

and De Meester 2024; Sriramulu et al. 2025), as illustrated in Supplementary fig. S1. Consistent with these models, observational studies have revealed rapid immune evolution following species' invasions (White and Perkins 2012; Cornet et al. 2016). However, most studies of perturbed host-parasite interactions (e.g., following invasions) take place long after new populations are founded, potentially missing transient early eco-evo dynamics.

Here, we present a test of eco-evolutionary dynamics in a host-parasite interaction between threespine stickleback (*Gasterosteus aculeatus*) and their specialist tapeworm, *Schistocephalus solidus*. We experimentally founded new populations of stickleback in nine natural lakes. Over the subsequent 6 years, we tracked changes in *S. solidus* infection rates and a key immune trait (fibrosis) in the newly founded populations, and in the eight native source lakes. We used this replicated long-term dataset to test seven hypotheses inspired by recent host-parasite eco-evo models (Fleischer et al. 2021; Sriramulu et al. 2025). First, parasite abundance should differ between source versus newly-founded host populations. In particular, the new populations may experience reduced parasite prevalence (enemy release) relative to the ancestral populations. Second, transplanted host populations should experience large temporal changes in parasite abundance as parasites spread (or decline towards extinction). Third, these ecological changes in parasite abundance should drive correlated changes in host immune traits (Fleischer et al. 2021). Fourth, many immune traits are inducible (plastic) responses to infection, but genotypes can vary in their baseline immune state or the magnitude of response (e.g., genetic variation in reaction norms). We therefore expected immune trait change would involve both heritable and plastic elements. Fifth, the newly founded populations should exhibit greater magnitude of fluctuations in infection and immune traits, compared to ancestral source populations that are more likely to be at equilibrium. Sixth, these fluctuations may dampen over time as new communities approach

their respective eco-evolutionary equilibria. Finally, if alternative stable states exist, the new populations may diverge from each other in immune traits, and infection rates. The results presented below are broadly consistent with these hypotheses, supporting our contention that the newly founded populations exhibit transient eco-evolutionary dynamics leading to population divergence.

METHODS

Study system: background on stickleback and *Schistocephalus* interactions

The threespine stickleback is a small north temperate coastal fish, widely used in studies of evolutionary ecology. The Diphyllbothriidean tapeworm, *Schistocephalus solidus*, is a strict specialist on threespine stickleback, the second of three hosts. *S. solidus* infects cyclopoid copepod, which are an important prey for stickleback. When an infected copepod is ingested, the tapeworm penetrates the fish's intestinal wall to grow in the body cavity among the organs, sometimes reaching >50% of its host's mass (Clarke 1954). Large parasite size facilitates predation by piscivorous birds, where the parasite completes its life cycle (Berger et al. 2021). Once in a bird's intestine, the parasite quickly mates and lays eggs that can hatch in freshwater to infect a new copepod. The tapeworm's generation time appears to be about one year, comparable to its stickleback host (1-3 years). Stickleback breed seasonally (each spring) and tapeworm infection rates appear to peak in the summer when bird activity and copepod abundance are highest (Heins et al. 2016).

Stickleback populations vary along an ecomorphological continuum. In large lakes, stickleback predominantly consume mid-water zooplankton (limnetic prey), while in smaller lakes they rely more on larger insect larvae (benthic prey). Stickleback populations have evolved

morphological features to adapt to these different diets: in larger lakes limnetic stickleback tend to have smaller gapes, more/longer gill rakers, and more fusiform body shapes, compared with the benthic stickleback in smaller lakes (Lavin and McPhail 1986; Willacker et al. 2010). This benthic-limnetic variation spans a continuum (not discrete types), varying among individuals within lakes (Matthews et al. 2010; Snowberg et al. 2015), between lakes (Lavin and McPhail 1986; Willacker et al. 2010; Bolnick and Ballare 2020), and between species pairs (Schluter and McPhail 1992; Schluter 1993; Arnegard et al. 2014). This ecomorphological and dietary variation is crucial to the host-parasite interaction. Limnetic stickleback consume more cyclopoid copepods, increasing their exposure to *S. solidus*. This diet-infection relationship holds within populations (Stutz et al. 2014), among populations (Bolnick et al. 2020), and between sympatric species pairs (MacColl 2009).

S. solidus infection is believed to be the most virulent of the many parasites affecting stickleback. The tapeworm can siphon >46% of the host's baseline metabolic output (Claar et al. 2023), reduce stickleback growth and fecundity (Barber and Scharsack 2010), and manipulate the fish to facilitate predation by birds. Therefore, selection should favor fish genotypes that resist *S. solidus* infection (or mitigate its effects). This expectation is confirmed by comparisons between marine and freshwater stickleback. The tapeworm does not survive in brackish water, so marine fish have not coevolved with the parasite, remaining highly susceptible. In contrast, when stickleback invade freshwater they rapidly evolve increased resistance (Weber et al. 2017a; Sriramulu et al. 2025). We expect this selection to be strongest in limnetic populations, because of their higher exposure risk (Stutz et al. 2014; Fleischer et al. 2021). Greater immunity in limnetic fish may suppress infection rates, obscuring the relationship between diet and exposure risk (Fleischer et al. 2021).

A major component of sticklebacks' immune response to *S.solidus* involves peritoneal fibrosis, though this is not the only immune pathway involved (Scharsack et al. 2004, 2007; Lenz et al. 2013; Fuess et al. 2021; Weber et al. 2022; Fuess et al. 2026). Fibrosis involves formation of extensive extracellular protein matrix (e.g., scar tissue) often associated with chronic inflammation (Henderson et al. 2020). In stickleback, fibrosis forms throughout the body cavity where the parasite develops, suppressing parasite growth and sometimes leading to tapeworm death (Weber et al. 2022). Fibrosis in stickleback is best viewed as a heritable reaction norm: the trait is induced by *S. solidus* exposure, but genotypes from different lakes vary in both baseline fibrosis and the magnitude of their induced response. Importantly, fibrosis is generally an irreversible lesion (Hund et al. 2022), lasting many months after a single parasite exposure, even if the parasite is rapidly eliminated. We have not found associations between fibrosis and other intraperitoneal parasites (e.g., *Glugea*, a microsporidian; or the nematodes *Anisakis* or *Eustrongylides*).

Multiple independent freshwater populations have evolved an increased fibrosis response to *S. solidus* compared to susceptible marine fish which lack fibrosis (Weber et al. 2022; Sriramulu et al 2025). This repeated evolution implies that fibrosis has adaptive value. However, fibrosis is also costly, reducing male and female fecundity, tissue flexibility, predator evasion, feeding success, and increasing metabolic expenditure (De Lisle and Bolnick 2021; Matthews et al. 2023; Sasser et al. In review). Due to these costs, some lake populations evolved to suppress fibrosis, favoring a strategy that tolerates infection (Weber et al. 2022). These population differences are heritable: a QTL mapping cross between a high- and a low-fibrosis population identified one locus on chromosome 2 that accounted for more than 30% of the variation in fibrosis in lab-exposed F2 hybrid stickleback. We still do not wholly understand the set of ecological (or historical) factors determining whether populations evolve fibrosis-based resistance, or fibrosis-suppression and

tolerance of *S. solidus*. The replicated experimental evolution study presented here provides an opportunity to test whether ancestry, or local environment, influence evolution of fibrosis.

Experimental design

In 2018, the Alaska Department of Fish and Game used a photodegradable toxin, Rotenone, to eliminate an invasive species of fish (Northern pike, *Esox lucius*) from nine lakes on the Kenai Peninsula, thereby eliminating all fish. Surveys in spring 2019 confirmed the lakes remained fishless. In May-June 2019, we used minnow traps to collect stickleback from eight native populations in nearby source lakes. Each fishless ‘recipient’ lake received a mixture of nearly equal numbers of founders from four source lakes (fig. 1A), with two exceptions detailed below. The mixed-population pools of founders created genetically diverse starting populations to facilitate subsequent adaptive evolution. A detailed rationale for the experimental design is given in (Hendry et al. 2024); the next two sections describe key aspects of our choices of source lakes, and recipient lake introductions.

Source lakes

Haines et al. (2023) identified eight lake populations of stickleback in coastal Alaska that varied along the class benthic/limnetic continuum of body morphology (Schluter and McPhail 1992; Matthews et al. 2010; Willacker et al. 2010; Bolnick and Ballare 2020; Haines et al. 2023). These genetically divergent populations (F_{ST} between 0.16-0.43; fig. 1B) were used as sources of founding fish for the experiment. Four of these lakes contained stickleback with relatively limnetic morphology, the other four populations were relatively benthic (Hendry et al. 2024). In general, stickleback in larger lakes tend to be more morphologically limnetic, while stickleback in smaller

lakes tend to be more morphologically benthic (Willacker et al. 2010; Bolnick and Ballare 2020). However, this correlation is noisy. In the eight particular lakes used here, lake size and ecomorphology were uncorrelated. Finger Lake has the largest surface area, but is shallow and contains morphologically benthic fish. Long Lake is small but deep and contains morphologically limnetic fish. We use morphology, not lake size, to define our set of four ‘benthic’ and four ‘limnetic’ source populations. Importantly, even stickleback from the small lakes have high genetic heterozygosity, providing substantial variation for selection to act upon in our experiment.

Experimentally founded populations

We generated new populations by moving fish trapped from the eight source lakes, into the nine newly fishless lakes (fig. 1A). The nine experimental lakes varied in size, including smaller ponds (benthic habitat), and larger lakes (limnetic habitat; supplementary fig. S2). Each lake received a mixture of stickleback transplanted either from the four benthic source lakes (benthic pool), or from the four limnetic source lakes (limnetic pool). This was done in a factorial design, such that benthic pool fish were added to two small lakes (benthic habitat), and two large lakes (limnetic habitat); the same held for the limnetic pool. A ninth recipient lake received an equal mixture of founders from all eight source lakes (benthic and limnetic). The recipient lakes are not connected by passable surface rivers to other stickleback populations, so natural recolonization is not a concern. We distributed a total of 10,831 stickleback among the nine newly-fishless recipient lakes. The number of fish added were scaled to lake size: the smallest two lakes each received ~420 fish, the largest two lakes received ~1650 fish each (table S1). By mixing fish from multiple source lakes, we sought to mitigate effects of genetic drift and maximize genetic variation for

selection to act on. But, we acknowledge that our founded populations harbor more genetic diversity than may be typical of naturally founded populations or new invasive species.

The transplants were conducted with IACUC approval (McGill University AUP 2000-4570) and permits from the State of Alaska (Aquatic resource permits SF2019-085, P-19-005) and Kenai National Wildlife Refuge (2019-Res-AHendry-6576).

Transplant success

Stickleback in Alaska can breed one year after hatching, although reproduction probably peaks in their second year of life. Our 2020 sample from the recipient lakes yielded many reproductively mature one-year-old fish, indicating that the introductions successfully established new populations. By 2021 population sizes were very large: setting just 10 minnow traps overnight along 20 meters of shoreline typically yielded over 1000 trapped fish per lake, comparable to source lake catch rates. Catch per unit effort has not changed detectably in most recipient lakes from 2021-2025. The exception was G Lake where colonists failed to breed: we captured few fish in 2020 and none in 2021. G lake is relatively limnetic habitat, and the benthic founders may have been maladapted. In 2022 we reintroduced a benthic and limnetic mix to G Lake, and the limnetic genotypes succeeded in establishing a large population (Eckert et al. 2026). We exclude G from most analysis here.

Sampling

In early June of each year we collected 100 stickleback per lake using minnow traps set overnight along the lakes shoreline. In 2019 we sampled stickleback from the eight source lakes just prior to introductions. Due to pandemic limitations, in 2020 we only sampled the recipient lakes. In 2021,

2022, 2023, and 2024 we sampled both source and recipient lakes. In 2025 we sampled only the recipient lakes. Exact sample sizes per lake and year are listed in supplementary table S2. Captured fish were euthanized in MS-222 and immediately dissected to acquire infection and fibrosis data. Sampling was done with IACUC approval (University of Connecticut A22-006) and permits from the State of Alaska (SF2020-103d, P-21-012, SF2022-043d, SF2023-030d, P-24-015, P-25-021).

Phenotypic measurements

We recorded weight and standard length from freshly euthanized fish. We dissected each fish to count *S. solidus*, determine sex from gonad morphology, and score fibrosis. Fibrosis was scored on an ordinal scale from 0 to 4 following protocols in Hund et al. (2022). A score of 0 means no fibrosis, the organs move freely separate from each other and from the body wall; 1 denotes moderate thread-like connections between organs, typically the liver to intestines; 2 indicates extensive connections between organs that can be separated by force; 3 is when organs are fully encased in a cocoon of fibrosis and cannot readily be separated without damage to the organs, and the organs are attached to the body cavity by fibrotic threads; 4 indicates the body wall cannot be separated from the organs without tearing the muscle tissue or organs. The visual fibrosis scoring is highly repeatable: independent observers' scores are highly correlated ($r > 0.95$; Bolnick et al. 2024). This fibrosis scoring is also correlated with biomechanical measures of tissue stiffness (Young's modulus) measured with an Optics11 Nanoindentor (Flanagan, unpublished results).

Ancestry inference

To test for evolutionary shifts in ancestry proportions in the recipient lakes, we genotyped individuals from the 2021 sample for single nucleotide polymorphisms (SNPs) diagnostic of each

source population. We used previously published PoolSeq data from the source lakes (Weber et al. 2022) to design two Fluidigm SNPtype arrays (Fluidigm Corporation, San Francisco CA), with 24 SNPs unique to each source population (one array for benthic source lakes, one for limnetic source lakes, supplementary table S3). We genotyped 95-97 fish from each of the recipient lakes in 2021, extracting DNA using a phenol-chloroform extraction protocol on caudal fin samples. For each individual, we computed the proportional ancestry descended from each source population (for details see Eckert et al, 2026). Assuming the generation time is at least one year, the 2021 sample could contain at most F2 generation individuals, so ancestry proportions are constrained to multiples of 0.25.

Breeding of fish for common-garden immune assays

To test for heritable differences in the fibrosis response among source lakes, we reared stickleback in a laboratory common garden setting, and exposed them to two immune challenges. In 2021 we sampled reproductively mature adults from the source lakes. We stripped eggs from gravid females, and fertilized these with sperm from dissected testes from males in the same population, generating within-population crosses, as described in (Stewart et al. 2017). In addition, we included two anadromous marine populations, Rabbit Slough and the Kenai River Estuary, representing ancestral character states for freshwater fish. Crosses were conducted with an Alaska Aquatic Resource Permit P-21-008. Embryos were shipped to the University of Wisconsin Madison and the University of Massachusetts Lowell for rearing in aquaria with previously described husbandry methods (Weber et al. 2022). Fertilized eggs were reared to maturity, grouped by family and housed at 17-19°C with an 18:6 hr light:dark cycle in a recirculating water aquarium

system. Rearing and the following experiments were done with approval from each institution's animal care committees (IACUC protocol numbers 21-10-07-Ste and L006460-A04 respectively).

Common-garden experimental infection

S. solidus were collected from infected threespine stickleback from Walby, Finger, and Tern Lakes in Alaska, and from Lake Kjerringøy in Norway (an allopatric population). Tapeworms were mated in vitro to generate eggs, as described in Weber et al. (2017a). The eggs were incubated in the dark at 18°C for 3-7 days before being exposed to light to induce hatching. *Acanthocyclops robustus*, a cyclopoid copepod, were fasted for 24 hours prior to being fed hatched tapeworm coracidia. Lab-raised fish from the source lakes were fasted for 24 hours to promote copepod consumption (University of Wisconsin Madison IACUC protocol number L006460-A04). Each fish was isolated and fed infected copepods. Exposures were done in two batches (sample sizes in supplementary table S4). In batch A, individual stickleback were fed 10-20 copepods that were infected with tapeworms from Walby, Tern, or Kjerringøy Lakes. Additional fish were fed uninfected copepods as a control. Fish were euthanized and fibrosis scored 41-48 days after exposure. In batch B (part of a separate experiment), fish were exposed to approximately 7-8 Walby Lake tapeworms (after 48 hours of fasting), and scored for fibrosis after 30 days.

Data Analysis

All of the following analyses were conducted using the R statistical language, version 2023.06.1+524 (R. Development Core Team 2022). R code is available on the data and code repository accompanying this paper.

Do source populations differ in infection prevalence and fibrosis severity?

We calculated the prevalence of *S. solidus* infections in each source lake, in each year (2019-2024, N = 2,748, table S2). Confidence intervals were calculated with the R package *exactci* v1.4-4 (Fay 2010). To test whether *S. solidus* infection rates differ between source lakes, we fit a general linear model testing for effects of lake, year, and a lake×year interaction on either infection prevalence (binomial GLM) with fish size (log standard length) and sex as covariates. Stable lake-to-lake differences should result in a large main effect of lake, and a relatively small contribution from lake×year interactions. Unstable infection rates should involve changes in rank orders of lake infections resulting in a large lake×year interaction effect. A large main effect of year would indicate region-wide fluctuations in parasite prevalence. We use the proportion of explained deviance to evaluate the temporal stability of between-lake differences. Throughout this paper, year is treated as a categorical factor in analyses, rather than presuming temporal change fits a linear trend. To test for ecological determinants of infection rate differences among source lakes, we fit a linear model testing whether *S. solidus* prevalence is related to log lake surface area, or fish ecotype (morphologically defined).

We used linear models to test for differences in fibrosis among source lake populations, with a model evaluating effects of lake, year, and a lake×year interaction, with fish log standard length and sex as covariates. We calculated Type II Sums of Squares and obtained P values using permutations because the fibrosis score is ordinal and so violates parametric assumptions. We have previously analyzed fibrosis data using cumulative links in Bayesian hierarchical linear models more directly designed for ordinal data. However, we consistently find that the cumulative link models agree with more intuitive linear models that are easier to present succinctly. Therefore for the purpose of this paper we opt to use the simpler regression model framework. We use the

relative percent variance explained by the model terms to evaluate whether population differences are temporally stable (e.g., main effect of lake is larger than lake×year interaction) or unstable (vice versa). Treating lakes as the level of replication, we used regression to test whether mean fibrosis severity is related to lake size, fish ecotype, and *S. solidus* prevalence.

Are the source population differences in fibrosis response heritable?

Previous laboratory infection experiments and field samples established that tapeworm infection induces fibrosis in stickleback from Vancouver Island, but the magnitude of this plastic response varies between genotypes (De Lisle and Bolnick 2021; Hund et al. 2022; Weber et al. 2022). Supplement A describes confirmation of this induced response using the data in this study. To test whether these responses differ between lakes, we challenged lab-reared fish from each source population with live infections or a standardized immune stimulant. For fish exposed to live tapeworms, we fit a linear model testing whether fibrosis varied as a function of fish population, tapeworm genotype, and their interaction. For fish given intraperitoneal injections, we fit a linear model seeking to explain fibrosis severity as a function of treatment (saline vs alum), population, and a treatment×population interaction. A significant population by treatment interaction would denote heritable differences in response to immune challenge. We used a correlation test to evaluate whether laboratory measures of mean fibrosis response were correlated fibrosis variation among source lakes in the wild-caught samples.

Testing the enemy release hypothesis: is tapeworm prevalence lower in recipient lakes?

We tested for differences in tapeworm prevalence between source versus recipient lakes using a binomial GLM with lake type (source/recipient), year, and lake type×year interaction. In this, and

following analyses, we treat the recipient lakes as independent populations. Shared ancestry of lakes receiving the same founder pools could initially create a degree of non-independence, but changes in each lake after founding represent independent eco-evo dynamics. The exception is a narrow connection between Hope and Rancho Lakes that allows gene flow between these two ecologically disparate lakes; as will be shown below, Hope and Rancho Lakes do diverge so this connection has little impact.

Does infection differ among recipient lakes, and among years?

We used binomial GLMs to test whether infection prevalence differs among recipient lakes, by year, or as a function of lake×year interactions (years 2020-2025, N = 4,298 fish). Fish sex and standard length were initially included as covariates. Standard length, in particular, could help detect potential confounding effects of age structure on infection status. However, neither sex nor standard length added appreciable explanatory power and so were dropped for brevity.

New populations founded by limnetic ecotypes might be more resistant to infection, if their ancestors had adapted to higher *S. solidus* exposure. Conversely, limnetic ancestry might predispose the new populations to consume more copepods, increasing exposure risk. Present-day environment may also affect infection rates: stickleback in larger recipient lakes might consume more zooplankton and have higher exposure rates. To estimate these effects of historical contingency (ancestry) versus ecology, we used planned contrasts within years to test whether infection prevalence in recipient lakes was related to lake type or ecotype ancestry (0%, 50%, or 100% limnetic populations in the founder pool).

To test for temporal auto-correlation in infection prevalence, we calculated the change in infection rate between each successive year, in each lake. As a stand-in for founder infection rates

in 2019, we used an expected prevalence calculated from the infection rates in source lake pools from 2019. We tested for correlations between prevalence each year, versus the between-year prevalence change (e.g., $\text{cor}(I_t, I_{t+1} - I_t)$). We tested similar temporal auto-correlations in source lakes.

Does fibrosis differ among recipient lakes, and among years?

We used linear regression to test for among-lake and among-year variation in fibrosis in the recipient lakes. The variance explained by lake main effect and lake×year interaction effect are used as a measure of the relative (in)stability of fibrosis through time. Sex and standard length were initially used as covariates to account for possible age structure within the recipient lakes, but these did not contribute appreciable effects and were dropped from further consideration. We then used estimates of the mean fibrosis for each population in a linear model to evaluate the effects of recipient lake habitat (benthic or limnetic) and ancestry (benthic or limnetic pool).

Is changing fibrosis in the recipient lakes consistent with reaction norm evolution?

We used the SNP array estimates of ancestry (2021 sample) to test for between-genotype differences in fibrosis in the recipient lakes. Specifically, do individual fish with greater ancestry from fibrosis-prone populations tend to have more fibrosis? Because each pool of founders was a mixture of four lakes, and each pool was added to four recipient lakes, we can partition the effects of ancestry, and present environment (lake, or lake type). Then, we ask whether these ancestry proportions change through time in the recipient lakes.

We used a Bayesian hierarchical linear model to estimate the effect of each source lake's genetic contribution to fibrosis in the recipient lakes in 2021. Predictors in the linear model

included lake (a random effect), fish standard length (covariate), and percent ancestry from each source lake. The model was fit with *stan* in R using the *rethinking* package (McElreath 2016), retaining posterior distribution means and 95% credible intervals. We tested a model including both a main effect of infection, and infection×ancestry interactions. WAIC model comparison identified the reduced models best fitting the data. To compare these field ancestry estimates against laboratory results, we tested for a correlation between source lake mean fibrosis (in lab-infections), and the mean posterior estimate of ancestry effects the recipient lakes.

To test whether evolution has occurred within each recipient lake, we use t-tests to compare mean ancestry proportions in 2021 against the expected proportion in the 2019 founder pool for that recipient lake (see Eckert et al 2026 for more detailed analysis). We test for correlations between the change in ancestry (from 2019 to 2021), and the resulting fibrosis severity in 2021. If fibrosis is due to selection on ancestry-dependent genotypes, we expect increased fibrosis to be associated with increased frequency of high-fibrosis source lake ancestry.

RESULTS

Infection prevalence and fibrosis differ among source lakes

The source populations differ in *S. solidus* prevalence (fig. 1C), ranging from 0% to 50% depending on the lake (binomial GLM lake effect Deviance = 389, df = 7, $P < 0.0001$). Likewise, fibrosis severity differed among source lakes (fig. 1D), ranging from an average of 0.21 to 1.23 (Kruskal-Wallis $\chi^2 = 458$, df = 7, $P < 0.0001$). A priori, we expected that *S. solidus* exposure rates should be higher in limnetic populations, which tend to consume more copepods (Bolnick and Ballare 2020). This expectation was not supported: for the eight lakes evaluated here, *S. solidus*

infection prevalence was unrelated to lake size ($t = 1.2$, $P=0.2787$) and fish ecotype ($t=-1.8$, $P=0.1194$).

The apparent absence of a relationship between ecological exposure risk and infection rate could be due to immune evolution. Models suggest that high risk populations (e.g., limnetic lakes) can evolve greater resistance, which suppresses rates of observable infections and obscures the relationship between diet, exposure, and infection (Fleischer et al. 2021). Consistent with this scenario, fibrosis was stronger in larger source lakes ($t=4.2$, $P=0.0082$, fig. 2A) where copepods typically form a larger diet share. Fibrosis was not reliably related to morphological ecotype ($t = 0.8$, $P = 0.4614$). Fibrosis can be high in lakes with few observable infections because it produces irreversible lesions that last many months after parasite exposure (Hund et al. 2022). In larger lakes, many fish may be exposed to *S. solidus*, triggering fibrosis that kills the tapeworm, resulting in a high frequency of fibrosis despite low prevalence of successfully established parasites.

The pools of fish used to found the experimental populations would have brought along different numbers of tapeworms. Although we did not find a generalizable effect of lake-level ecotype on lake-level infection ($N = 4$ lakes per ecotype), there are strong population differences in infection prevalence. As a result of these differences, an equal mixture of fish from the four benthic lakes used here is expected to have a 3-fold higher infection prevalence (0.185) than a mixture of fish from the four limnetic lakes (0.060; $P<0.0001$). The benthic pool includes heavily-infected Walby and Finger Lakes, whereas the limnetic pool included two lakes with negligible prevalences (Long and South Rolly).

Fibrosis responses differ heritably among source lakes

Previous experiments showed that tapeworms stimulate a plastic fibrosis response. Confirming this result, within most source lakes fibrosis was higher in infected individuals than in uninfected individuals (fig. 2B; details in Supplement A). But, this difference was especially strong in some lakes (8.2-fold difference in South Rolly) and non-significant in others (1.1 fold-change in Walby). By experimentally exposing lab-raised stickleback to controlled doses of *S. solidus*, we confirmed these between-population differences in fibrosis response are heritable. Fibrosis in cestode-exposed lab-raised fish varied among source populations (fig. 2C, $F_{7,196}=10.3$, $P<0.0001$) as well as by tapeworm strain (fig. S3). The fibrosis response to laboratory cestode exposure was stronger in fish bred from larger lakes ($r=0.851$, $P=0.032$). This observation is consistent with our expectation that populations in larger lakes have higher exposure to *S. solidus* and therefore evolve greater fibrosis-based resistance. The laboratory response to experimental infection was positively correlated with fibrosis severity in wild-caught fish from the source lakes ($r = 0.752$, $df = 5$, $P = 0.0513$). In contrast, all source lakes responded with equal fibrosis to an artificial stimulant (fig. S4), suggesting the reaction norm variation is due divergent responses to *S. solidus* antigens.

This heritable variation among source lakes implies that each pool of founding fish transplanted into the recipient lakes harbored genetic variation in fibrosis response that selection might act upon. But, genetic variance in fibrosis was not equal between the ecotype pools. Using fibrosis scores from the infection experiment (fig. 2C), individual fish fibrosis averaged 0.54 with a variance of 0.81. Variance among the four benthic lakes' means was 0.31, compared to a variance of 0.06 among the four limnetic source lakes. Consequently, the benthic pool had 5.3-fold higher among-population variance in mean fibrosis response, because it included non-fibrotic Walby

Lake fish, and highly fibrotic Finger Lake fish. Within-lake fibrosis variances ranged from 0.11 (Walby) to 1.37 (Finger).

Recipient lakes initially exhibit enemy release

Consistent with the enemy release hypothesis (Boyce et al. 2011; Schatz and Park 2023), from 2021-2024 the prevalence of *S. solidus* infection was on average 77% lower in recipient lake populations than in their ancestral source lakes in the same year (fig. 3; release effect $F_{1,54}=10.67$, $P = 0.001$). Similarly, infection intensity averaged 0.091 in recipient lakes from 2021-2024, compared with 0.449 in source lakes over the same period, an 80% reduction (release effect $F_{1,54}=8.29$, $P = 0.0057$). The magnitude of this release declined in later years (release \times year interaction $F_{1,58}=3.22$, $P = 0.0778$; year treated as a numerical predictor here to detect a directional trend). This reflected increasing infection rates especially in recipient lakes, which could either result from within-lake parasite population growth or immigration via piscivorous birds.

Recipient lakes exhibit large temporal fluctuations in infection

Within the long-established source lake populations, infection prevalence was relatively stable across years (fig. 4A). A binomial GLM with lake, year, and lake \times year interaction explained 37.5% of the total deviance in *S. solidus* infection prevalence. Persistent among-lake differences contributed most of this variation (main effect of lake contributed 72.8% of explained deviance, $P<0.0001$). The main effect of year was significant but relatively weak (19.6% of explained deviance; $P<0.0001$), suggesting there are region-wide shifts in parasite abundance from year to year. Generally, the infection prevalence in different lakes stayed relatively constant: although the lake \times year interaction effect was significant ($P<0.0001$) it contributed only 7.7% of the explained

deviance. This weak interaction is reflected in the stable rank orders of lakes over time (fig. 4A): Walby Lake had the highest infection prevalence in all five years for which we have data, whereas Long Lake and South Rolly Lake consistently had the lowest prevalence. We infer that, over the six years that we sampled source lakes, these populations were approximately at ecological equilibria with their *S. solidus* parasites.

The newly founded recipient lake communities should be far from an eco-evolutionary equilibrium. The stickleback populations consist of new combinations of host genotypes, in a new environment, with reduced parasite abundance fig. 3 and perhaps unfamiliar *S. solidus* genotypes. We therefore expect infection rates to fluctuate substantially within each lake as the parasite population reproduces and host immunity evolves. Consistent with this expectation, infection prevalence fluctuated strongly among years within the recipient lakes (fig. 4B). A binomial GLM with lake, year, and lake×year interaction explained 21.1% of the total deviance in *S. solidus* infection prevalence, most of which was due to a lake×year interaction effect (46.3% of explained deviance; $P < 0.0001$), nearly twice as large as the main effect of year (26.3%; $P < 0.0001$) or lake (27.4%; $P < 0.0001$). This large interaction effect indicates large changes in relative infection rates among lakes, through time, consistent with destabilized host-parasite interactions. In 2019 the benthic pool of founding fish arrived in their new lakes carrying on average 3-fold more *S. solidus* (e.g., based on the prevalences in the eight lakes, a mixed pool of benthic fish would be more heavily infected because they include the high-prevalence Walby lake fish). However, by the following year these between lake differences had reversed: infection rates were highest in lakes receiving the limnetic founders ($t = 2.77$, $P = 0.0323$). By 2023 the relationship flipped again, with higher prevalence in lakes receiving benthic founders ($t = -2.011$, $P = 0.0901$). Although these specific contrasts were done post-hoc, they illustrate a broader point that infection prevalence

fluctuated greatly within lakes, and rank-order differences among lakes frequently reversed. These unstable host-parasite dynamics in recipient lakes contrast starkly with the relative stability in source lakes. These changes are not likely to be attributable to age structure differences between lakes, given that body size was not significantly associated with infection status in the GLM ($P=0.4078$). Prevalence dynamics apparently stabilized after six years: rank order infection differences were largely unchanged from 2024-2025, remaining consistently higher in lakes that received limnetic pool founders ($P = 0.001$).

Fibrosis is relatively stable in source lakes but fluctuates over time within recipient lakes

Like the infection temporal trends, the source lakes exhibit relatively stable differences in fibrosis (fig. 4C), whereas fibrosis fluctuated over time within recipient lakes (fig. 4D). In the source lakes, fibrosis scores differed by lake (65.2% of explained variance, $F_{7,2339}=104.0$, $P<0.0001$), and year (20.4% of explained variance, $F_{4,2339}=56.9$, $P<0.0001$), along with a comparatively small lake \times year interaction (14.4%, $F_{25,2339}=6.4$, $P<0.0001$; model explaining 47.7% of the overall variance). In contrast, in the newly founded populations (fig. 4D) between-lake differences were weaker (21.4% of explained variance, $F_{8,4157}=70.2$, $P<0.0001$). Fibrosis varied among years for all recipient lakes (main effect of year, 64% of explained variance; $F_{4, 4157}=336.5$, $P<0.0001$), but there was also a lake \times year interaction (14.5% of explained variance, $F_{27,4157}=10.9$, $P<0.0001$; overall model explained 39% of the variation). This interaction tells us that fibrosis differed among the newly founded lakes, but these among-lake differences changed over time. Specifically, a post-hoc analysis of recipient lakes revealed that among-population variance in fibrosis was initially weak but increased over the five years of the study ($r = 0.86$, $t = 3.4$, $df = 4$, $P = 0.027$). These results indicate that, over time, the new population diverged from each other in fibrosis levels.

The emerging differences in fibrosis among reintroduced populations reflects effects of both their ancestry and present habitat. We expected fish descended from the limnetic source lakes to have inherited a greater capacity for fibrosis. Lakes populated by limnetic founders exhibited consistently stronger fibrosis than those receiving benthic founders in basically all years. For example, in 2025 populations descended from limnetic founders had 3.8-fold stronger fibrosis on average (fig. 4D, $t=-9.6$, $p < 0.0001$) than benthic-founded lakes. The lasting effect of founder ecotype on subsequent fibrosis, replicated across ecologically varying lakes, reveals an important effect of historical contingency in the distribution of this heritable immune trait.

We also expected fish in larger lakes to consume more copepods, leading to higher *S. solidus* exposure, which should induce stronger fibrosis. This expectation received inconsistent support. In 2023, fibrosis was indeed significantly stronger in larger limnetic recipient lakes than in smaller lakes ($F_{1,4}=79.9$, $P=0.0009$), controlling for ancestry. However, lake size had no effect in 2024 ($P = 0.691$). In 2025 fibrosis was marginally higher in the smaller benthic lakes ($P = 0.0624$), contradicting our initial predictions. From these observations we conclude that fibrosis in the recipient lakes reflects both persistent effects of historical contingency (i.e., which genotypes first founded the populations) and temporally varying effects of present-day habitat.

Coupled changes in infection and fibrosis over time

We observe temporal correlations between infection rates and immune traits, consistent with models of eco-evolutionary dynamics (Fleischer et al. 2021; Buckingham and Ashby 2022; Yamamichi 2022). Theory suggests that when infections are common, selection should favor greater immunity that then suppresses suppress infection rates. When infections are rare, selection may favor the loss of costly immune defenses (Lochmiller and Deerenberg 2000), enabling

subsequent increases in parasite abundance. This can lead to a cyclical change in infection and immunity, visible on a phase plane diagram (fig S1; Sriramulu et al. 2025). Supplement B presents the dynamics from the source and recipient lakes on a comparable phase plane. This visualization approach not only highlights the larger year-to-year changes in the recipient lakes compared to source lakes (Supplement B fig. S.B.2), but also reveals that the source lakes approximately conform to the counter-clockwise eco-evolutionary trajectory arising from a recent theoretical model (fig S1).

In the first generation after reintroduction (2020), lakes with more tapeworm infections tended to have higher mean fibrosis ($r=0.85$, $df = 7$, $P = 0.015$; fig. 5A). This positive relationship is consistent with the notion that having infection induces a plastic fibrosis response. This among-lake trend matches the positive within-lake association between infection and fibrosis (Supplement A). The among-lake relationship retained a similar slope, though marginally non-significant, in 2021 ($r=0.63$, $P = 0.093$) and 2022 ($r=0.60$, $P = 0.116$). However, the relationship disappeared in 2023 ($r=-0.09$, $P = 0.779$) and reversed entirely in 2024 ($r = -0.76$, $P = 0.027$) and 2025 ($r = -0.74$, $P = 0.021$). In these later years, lakes with the highest fibrosis had fewer viable tapeworm infections (even though within lake associations remained positive, Supplement A). As a result, from 2020 to 2025, among-population correlations between infection and fibrosis began strongly positive, and shifted to strongly negative (supplementary fig. S5, $r = -0.954$, $P = 0.003$, a post-hoc analysis).

Why might this infection-fibrosis relationship change? Theory has shown that this progressive decoupling, then reversal, of the infection-fibrosis relationship can occur if high-exposure populations evolved a strong inducible fibrosis response. This stronger response (or, an increased baseline) can suppress observable infection rates, while the irreversible fibrosis lesions

persist in exposed but resistant individuals (Sriramulu et al. 2025). Consistent with this model, mean fibrosis rates increased in all the recipient lakes over the span of the study (fig. 4D), suggesting possible evolution of a stronger constitutive or inducible response. The weaker fibrosis response observed in 2020-21 may have been insufficient to suppress the tapeworm population, while the later stronger response may have crossed a threshold and begun to effectively limit infection rates.

Because fibrosis suppresses *S. solidus* viability (Weber et al. 2017b, 2022), we expected to find that populations with high fibrosis in one year exhibited a subsequent decline in *S. solidus* prevalence (from year t to $t + 1$). This prediction was confirmed in some between-year intervals in 2020-21 ($r = -0.77$, $P=0.0427$) and 2022-23 ($r=-0.652$, $P=0.0798$; fig. 5B). However, this relationship did not hold in other time intervals (2021-22 $r = -0.05$, $P = 0.91$; 2023-24 $r = -0.21$, $P = 0.614$; 2024-25 $r = 0.65$, $P = 0.082$). As a result, there was a significant interaction between year and initial fibrosis ($F_{5,36}=12.4$, $P<0.0001$), but an overall negative trend that is consistent with our expectations.

If infection induces (or, selects for) an immune response that subsequently limits infections, the tapeworms should show negative density-dependence. This should result in a negative auto-correlation between infection prevalence (in year t) and the subsequent change in prevalence (from t to $t+1$). We observe this negative auto-correlation in the recipient lakes (fig. 5C; main effect of initial infection $F_{1,37}=106.9$, $P<0.0001$) for most between-year changes (2019-20: $r = -0.92$, $P = 0.0005$; 2020-21: $r = -0.97$, $P < 0.0001$; 2022-23: $r = -0.81$, $P = 0.0138$; 2024-25: $r = -0.63$, $P = 0.0933$), but not in 2021-22 and 2023-24 (both $r<0.1$ and $P>0.9$). The varying correlation led to a significant interaction between year and prior prevalence ($F_{5,37}=5.6$, $P=0.0006$). Interestingly, although the source lakes showed far weaker inter-annual changes in infection, they

also exhibit tapeworm negative density dependence (main effect of prior prevalence, $F_{1,17}=8.4$, $P = 0.01$; from 2021-22 $r = -0.62$, $P = 0.134$; 2022-23 $r = -0.97$ $P=0.0002$, and 2023-24 $r = -0.84$, $P = 0.017$).

Heritable variation in infection and fibrosis within recipient lake populations.

Do these changes in parasite prevalence and fibrosis reflect ecological changes alone, or does evolution contribute? We cannot yet definitively answer this question, but several lines of evidence suggest variance in fibrosis is heritable, connected to infection, and that this immune trait evolved in the recipient lakes.

Each lake received a mixture of source lake genotypes, and the same mixtures were replicated across multiple lakes. This allows us to statistically partition genetic and environmental effects on individual infection and fibrosis, using the SNP array to estimate individual ancestry in 2021. A Bayesian hierarchical linear model (controlling for fish size and recipient lake) indicates that fibrosis tends to be higher in fish with more Finger or Long Lake ancestry, and lower in fish with Walby Lake ancestry (fig. 6A). Within the recipient lakes, individual fish with *S. solidus* infection tend to have higher fibrosis than individuals without (Supplement A). The magnitude of this response depended on individuals' ancestry (supplementary fig. S7). For example, fish with more Walby Lake ancestry (low fibrosis) showed a weaker fibrosis response to infection within the recipient lakes. Conversely, ancestry from high-fibrosis Finger Lake conferred a stronger fibrosis response to infection. Remarkably, these effects of ancestry within recipient populations in nature were positively correlated with fibrosis severity in the original source lakes (fig. 6B, $r=0.752$, $P=0.051$) and with the fibrosis responses of lab-reared source lake fish after tapeworm exposure (fig. 6C, $r=0.864$, $P=0.012$). This consilience of several lines of evidence confirms there

is heritable variation in fibrosis among source lakes, and as a result there is heritable variation within recipient lakes. Ancestry also affects individual stickleback's probability of carrying a *S. solidus* infection (supplementary fig. S8). This evidence for heritability of infection could be due to either genetic variance in ecomorphology affecting diet and exposure rates, or due to variation in immunity.

We confirmed that there is rapid evolution in the recipient lakes: the ancestry frequencies shifted appreciably between the original introductions in 2019 and 2021 (Eckert et al. 2026). To present two examples, the frequencies of both Walby Lake ancestry, and South Rolly Lake ancestry, changed significantly from 2019 to 2021 (fig. 7A&B). The changes in ancestry frequencies in the recipient lakes were in many cases too large to be explained from initial founder effects, drift, and sampling error alone (fig. S9), implying an effect of selection. Moreover, certain source lake genotypes increased (or decreased) in frequency in parallel across multiple recipient lakes. For instance Long Lake ancestry increased in frequency in all four benthic pool recipient lakes, while Spirit Lake ancestry declined in all four (Eckert et al. 2026). In limnetic pool recipient lakes, Watson and Walby lakes consistently increased while Tern and Finger decreased (Eckert et al. 2026). Such repeatability is strong evidence for selection rather than drift.

These evolutionary changes in genotype frequencies are correlated with shifts in fibrosis severity. For example, recipient lakes with increasing Walby ancestry exhibited lower fibrosis than other lakes ($r = -0.73$, $P = 0.0388$; fig. 7C). This trend matches evidence presented above, that Walby Lake fish have very low fibrosis in the lab, and in the field. Conversely, increases in South Rolly ancestry are positively related to fibrosis in 2021 ($r = 0.81$, $P = 0.0155$; fig. 7D). This result is puzzling as South Rolly fish tend to have low fibrosis in their original lake, in the lab, and South Rolly ancestry confers slightly reduced fibrosis in recipient lakes. We emphasize that these

correlational results rely only on genome-wide ancestry rather than changes at particular genes; and only in one year. More detailed analyses of gene-level evolution and fibrosis GWAS will be presented in future papers and may help resolve the nature of fibrosis evolution.

Discussion

Newly founded populations are promising systems to study eco-evolutionary dynamics, because they may initially be far from any eco-evolutionary equilibria. New populations often experience ‘enemy release’ from parasites or predators (Elton 1958; Keane and Crawley 2002; Liu and Stiling 2006; Schatz and Park 2023). This initial release may be followed by ecological changes in parasite abundance as local parasite species (or genotypes) begin to exploit the new host population. Similarly, the new host population may be far from a local phenotypic optimum, and consequently undergo rapid evolution. For instance, parasite release can favor the evolution of reduced immunity to minimize costs of an unneeded trait (Cornet et al. 2016). We therefore expected that newly established populations will exhibit strong eco-evolutionary dynamics, such as coupled changes in parasite infection and host immunity. These fluctuations may dampen with time as populations approach new equilibria. In contrast, long-established populations are more likely to be at, or near, eco-evolutionary equilibria, making eco-evo dynamics hard to detect. Our experiment, which founded 9 new lake populations of stickleback, yielded infection and immune dynamics that largely supported these expectations.

Enemy release in recipient lake populations

Most tests of the enemy release hypothesis have been observational, taking advantage of existing cases of species invasion or range expansion. These comparative tests often take place long after

the initial founding event, and generally lack independent replicates. We are able to confirm partial enemy release in a replicated experiment. *S. solidus* infection prevalence and intensity were lower in the recipient lakes than in source lakes in the first few years (first few stickleback generations) after transplantation, though the parasite was not wholly lost. This release effect decayed over time and by 2025 there was no difference between source and recipient lakes.

A relevant question is, where did the recipient lake *S. solidus* come from? Some would surely have been carried to the empty lakes by infected founding fish, but eggs may also have been deposited into the lakes by passing birds (the terminal host). This external input of parasites may have accelerated as the repopulated lakes began to attract more piscivorous birds. Anecdotally, people living by the recipient lakes reported an uptick of breeding loons, mergansers, and goldeneyes. Future work on tapeworm phylogeography could help identify the source(s) of the tapeworm populations.

Destabilized host-parasite interactions in reintroduced populations

The native source lakes exhibit relatively stable between-lake differences in infection (fig. 4A), and fibrosis (fig. 4C). Among-lake differences are much larger than the lake \times year interactions, from which we infer the source lakes are close to eco-evolutionary equilibria. In contrast, the recipient lake populations exhibit unstable infection dynamics (large lake \times year interaction effects). A high-infection lake one year might be a low-infection lake the next year (fig. 4B). These initially large fluctuations weakened with time. By the final years of the study (2024-2025) the between-year variation weakened and among-lake variation increased (Fig. 4D). This declining temporal variability leads us to infer that the new populations may already be approaching new equilibria, with different lakes approaching different immune strategies.

The key source of the unstable dynamics in the recipient lakes was a temporal negative auto-correlation in *S. solidus* abundance. Lakes with high *S. solidus* prevalence in one year exhibited a subsequent decline in *S. solidus* prevalence in the following year, whereas low-infection lakes exhibited increases in prevalence (fig. 5C). We observe this negative density-dependence for the parasite in most years, in both source and recipient lakes. Such negative frequency-dependence can arise when high parasite abundance drives increased host immunity (through evolution or plasticity), subsequently suppressing infections (Koskella 2018; Fleisher et al. 2022). Consistent with this expectation, we repeatedly find that infection is associated with increased fibrosis in individual fish (Supplement A). As the experiment progressed, however, fibrosis increased across the recipient lakes, until it began to suppress infections: by 2024 and 2025, the most heavily fibrotic populations had fewer viable parasite infections. As a result, each population traverses a range of combinations of infection and fibrosis over time (Supplement B). However, the new populations' trajectories through infection-fibrosis space generally do not follow a single clear direction or arc. In contrast, the relatively (but not entirely) stable source lakes do exhibit the counter-clockwise arcs through infection-fibrosis space (Supplement B) expected from theory (fig S1). This counter-clockwise arc of increasing infection, then fibrosis, then suppressed infection, has also recently been documented in two other stickleback populations, following introduction of marine stickleback to a quarry pond in 1968 (Sriramulu et al. 2025), and following adaptive introgression into a native lake (Flanagan et al. 2025).

Although the experimental populations have only been changing for six years, shifts in infection prevalence and fibrosis suggest strong and persistent effects of historical contingency (founder genotypes). In addition, there are clear effects of local habitats within the new populations, though this is weaker than ancestry effects. Our *a priori* expectation was that the

populations founded from limnetic sources would tend to contain more pro-fibrotic genes, due to their evolutionary history of a higher intake of limnetic copepods, *S. solidus*' first host. Consistent with this expectation, populations founded from limnetic ancestors exhibited stronger fibrosis (fig. 4D). This difference increased over time, suggesting that limnetic populations either experienced stronger selection for high fibrosis, or an increased plastic response to higher exposure rates. Common garden infection experiments or genetic mapping of fibrosis will be required to resolve these alternatives in the future. We also see higher fibrosis in larger recipient lakes, consistent with our *a priori* expectation that stickleback inhabiting more 'limnetic' habitats will tend to consume more copepods, encounter more *S. solidus*, and either evolve or be induced to have more fibrosis. Theory suggests that ecomorphology may tend to evolve especially quickly to suit local resources, followed by immune evolution (Fleischer et al 2022). This lag is because initially the new population may be a generalist faced with multiple parasites requiring conflicting immune strategies. Only when the population has begun to specialize on a particular diet will immune traits subsequently evolve to impart resistance to whichever parasites are most often associated with that diet. To test this model, a next step will be to analyze evolution of ecomorphology, and changing diets, within these lakes to gain a better understanding of shifts in parasite exposure risk.

Eco-evolutionary dynamics?

The most challenging question is whether the infection and fibrosis dynamics described here are purely ecological (changes in parasite abundance), or whether they also entail evolutionary changes that represent an example of eco-evolutionary dynamics. Some circumstantial evidence leads us to infer that eco-evolutionary processes are operating. First, we know that fibrosis is induced by infection (Hund et al 2021; Supplement A), but the magnitude of this change differs

heritably among populations. For instance, in a cross of two lake populations from Vancouver Island, a single large effect QTL contributed over 30% of the observed variation in fibrosis (Weber et al. 2022). Our results confirm that fibrosis differences exist among populations in Alaska, and these are heritable. The immune differences between source lakes persist in artificially infected lab-raised fish, and persist as ancestry effects in the recipient lakes. For instance, Finger, Spirit, and Wik Lake fish exhibit higher fibrosis both in nature and the lab; their descendents also have higher fibrosis in the recipient lakes. This corroboration between lab and field effects reveals a repeatable genetic effect even across radically different environmental contexts. We are therefore highly confident that fibrosis is heritable.

We cannot yet entirely rule out the possibility that changes in fibrosis over time are a result of changing parasite exposure. If parasite encounter rates increased, more fish may be stimulated to initiate fibrosis (irreversibly), leading to an increase in observed fibrosis without requiring any evolution. However, genotyping our 2021 samples confirmed that evolution has occurred within the first generations of the experiment: some source lake ancestries became more common (others less common), within each of the recipient lakes, relative to the frequencies that we introduced (fig. 7A&B). We infer that this evolution was a result of natural selection, being too large to be explained by drift. We also observe some parallelism in the genotype frequency changes among lakes (see Eckert et al. 2026 for details), further supporting natural selection.

The resulting divergence in genotype frequencies among lakes is associated with divergence in fibrosis. Walby Lake stickleback have the lowest fibrosis of all source lakes (in the wild, and in the lab). In the recipient lakes, populations with increasing Walby ancestry had the lowest fibrosis (in 2021). Increased South Rolly Lake ancestry was associated with increased fibrosis, which is more difficult to explain as South Rolly was not originally a high fibrosis

population. But, these associations between changing genotype frequencies and changing fibrosis is largely consistent with our inference that fibrosis is evolving. Importantly, ancestry per se may not be a sufficient reflection of changes at particular genes that regulate fibrosis. Ongoing genotyping of additional years will allow more definitive GWAS mapping fibrosis to particular loci, and may reveal evolution of allele frequencies at those loci.

We acknowledge that there may be alternative hypotheses to explain our observed trends. First, we need to consider the potential role of genetic drift, and correlational selection. Our initial founding population sizes ranged from ~400 to 1600 individuals. Nonetheless, genetic drift surely contributes to modest changes in ancestry and phenotypes through time (fig. S9). But, the magnitude of genotype changes and the parallel changes among lakes strongly suggests selection is operating. However, selection could in principle be acting on a linked or pleiotropic trait, rather than on the immune role of fibrosis per se. Or, the fibrosis changes may be a result of tapeworm evolution, as different genotypes of *S. solidus* have different protein antigens (Wang and Bolnick 2025) and induce different levels of fibrosis (Bolnick et al. 2025).

We must also consider some non-evolutionary hypotheses. Between-year changes in fibrosis trait means (and infection rates) might arise from demographic differences between groups ('class structure'). For instance, if tapeworm infected individuals have elevated mortality rates then within a cohort we could see declining parasite prevalence through time without requiring natural selection on genotypes (Taylor 1990; Grafen 2015; Lion 2018). Class structure can also be introduced by the irreversible nature of the fibrosis response: temporal variation in *S. solidus* abundance in copepods will affect stickleback exposure rates, and thus the frequency of fibrosis. Finally, there may be stochastic variation in parasite prevalence: newly founded host-parasite populations might be inherently more demographically variable. However, this should not produce

systematic associations between fibrosis and parasite prevalence, nor such clear density-dependence for the parasite. We had similar sample sizes in source and recipient lakes, and population sizes in the latter quickly grew to equal or surpass source lake abundances (judging by high capture rates even in 2020).

We envision several important future steps to solidify our conclusions about fibrosis evolution and eco-evolutionary feedbacks. First, we will need to replicate the experimental infection and injection assays using lab-raised recipient lake fish, to confirm that divergent evolution led to heritable between-lake differences among our experimental populations. Second, we are completing genome-wide genotyping of all sampled recipient lake fish in all years, to allow locus-level measures of selection and genetic mapping of fibrosis and infection. We predict that GWAS loci affecting fibrosis will exhibit signatures of selection.

Conclusions

Our replicated whole-lake experiment allowed us to document the very earliest stages of host-parasite dynamics in multiple newly founded populations. The resulting data shows that parasite load (at least for *S. solidus*) is significantly reduced in the new populations. This reduction is followed by large temporal fluctuations in both infection and a key immune trait, intraperitoneal fibrosis. Fibrosis is regulated by a genotype \times environment interaction, so changes over time might reflect evolution or shifting parasite exposure. But, we can confirm that genotype frequencies are evolving within the experimental lakes, and that changes in ancestry are associated with shifts in fibrosis. From these observations we infer that eco-evolutionary dynamics are unfolding in the early generations of these new populations. Specifically, we have been able to document rapid, coupled changes in infection and immunity in the earliest generations of newly founded

populations. These rapid changes would be overlooked by observational studies of well-established invasive species, which are often studied years after an initial invasion. Because parasitism has a large impact on population viability, the eco-evolutionary dynamics documented here may play a key role in the early success or failure of invasive species (Martin et al. 2017; Weber et al. 2017a), geographic range expansion under climate change, and species reintroductions for conservation (Olden et al. 2011; Gross et al. 2024).

Acknowledgments

This research was made possible with support from the Alaska Department of Fish and Game, with particular thanks to Robert Massengill. The initial 2019 survey of source lake fish was carried out with help from Christopher Peterson, Trey Sasser, Elsa Dikko Tiya, Kelly Ireland, and Rachel Kramp. The transplants were conducted with help from Hilary Poore, Luis Baertschi, Matt Josephson, Christopher Peterson, Ismail Ameen, Anya Mueller, Chelsea Bishop, Victor Frankel, Allegra Pearce, Matt Walsh, and Michelle Packer. Resampling from source and recipient lakes in later years was done with help from Andrea Roth, Maria Rodgers, Arshad Padhiar, Annika Wohlleben, Kevin Newmann, Kelly Ireland, Emily Kerns, Saraswathy Vaidyanathan, Steve Bezdecny, Rogini Runghen, Sarah Pasqualetti, Abdoleman Nouri, and Benjamin Sulser.

Funding: Funding to conduct this work was provided by the US National Science Foundation (grants DMS-1716803 to DIB; FAIN-2133740 to DIB), US National Institutes of Health (grants R35GM142891 to JNW; R15GM122038 to KMM), Swiss National Science Foundation (grant TMAG-3_209309 to CLP), the Chan Zuckerberg Initiative Science Diversity Leadership (grant 2022-253562(5022) to KMM), and startup funds from the Universities of

Connecticut (DIB, KMM), Alaska Anchorage (JNW), Wisconsin Madison (JNW), and Massachusetts Lowell (NCS).

Competing interests: Authors declare that they have no competing interests.

Statement of Authorship

Conceptualization by APH, DIB, RDHB, KMM, CLP, JNW, NCS, and GH. Methodology by DIB, RDHB, APH, KMM, CLP, JNW, and NCS. Investigation by DIB, RDHB, LE, APH, EVK, ÅJL, KMM, CLP, KS, KTS, ART, CW, JNW, NCS, and GH. Visualization by DIB and EC. Funding acquisition by DIB, KMM, CLP, JNW, and NCS. Project administration by APH and DIB. Supervision by DIB, JNW, NCS, and KMM. Writing of original draft by DIB. Review & editing of writing by all authors.

Data and materials availability

All data files and R code required to reproduce the results in this paper have been archived at Figshare.org, DOI: [10.6084/m9.figshare.26093566](https://doi.org/10.6084/m9.figshare.26093566) (Bolnick 2024).

Literature Cited

- Arnegard, M. E., M. D. McGee, B. W. Matthews, K. B. Marchinko, G. L. Conte, S. Kabinr, N. Bedford, et al. 2014. Genetics of ecological divergence during speciation. *Nature* 511:307–311.
- Barber, I., and J. P. Scharsack. 2010. The three-spined stickleback- *Schistocephalus solidus* system: an experimental model for investigating host-parasite interactions in fish. *Parasitology* 137:411–424.
- Berger, C. S., J. Laroche, H. Maaroufi, H. Martin, K.-M. Moon, C. R. Landry, L. J. Foster, et al. 2021. The parasite *Schistocephalus solidus* secretes proteins with putative host manipulation functions. *Parasites & Vectors* 14:436.

- Bolnick, D. I. 2024. Data and Code Repository for: Destabilized host-parasite dynamics in newly founded populations. figshare. Dataset. <https://doi.org/10.6084/m9.figshare.26093566.v5>
- Bolnick, D. I., S. Arruda, C. Polania, L. Simonse, A. Padhiar, M. L. Rodgers, and A. J. Roth-Monzón. 2024. The dominance of coinfecting parasites' indirect genetic effects on host traits. *American Naturalist* 204:482–500.
- Bolnick, D. I., and K. M. Ballare. 2020. Resource diversity promotes among-individual diet variation, but not genomic diversity, in lake stickleback. *Ecology Letters* 23:495–505.
- Bolnick, D. I., E. J. Resetarits, K. Ballare, Y. E. Stuart, and W. E. Stutz. 2020. Scale-dependent effects of host patch traits on species composition in a stickleback parasite metacommunity. *Ecology* 101: e03181
- Boyce, W. M., M. E. Weisenberger, M. C. T. Penedo, and C. K. Johnson. 2011. Wildlife translocation: the conservation implications of pathogen exposure and genetic heterozygosity. *BMC Ecology* 11:5.
- Buckingham, L. J., and B. Ashby. 2022. Coevolutionary theory of hosts and parasites. *Journal of Evolutionary Biology* 35:205–224.
- Claar, D. C., S. M. Falad, N. C. Mastick, R. L. Welicky, M. A. Williams, K. T. Sasser, J. N. Weber, et al. 2023. Estimating the magnitude and sensitivity of energy fluxes for stickleback hosts and *Schistocephalus solidus* parasites using the metabolic theory of ecology. *Ecology and Evolution* 13:e10755.
- Clarke, A. S. 1954. Studies on the life cycle of the pseudophyllidean cestode *Schistocephalus solidus*. *Journal of Zoology* 124:257–302.
- Cornet S., Brouat, C., Diagne, C. and N. Charbonnel. 2016. Eco-immunology and bioinvasion: revisiting the evolution of increased competitive ability hypotheses. *Evolutionary Applications* 9:952-962.
- Cortez, M. H., S. Patel, and S. J. Schreiber. 2024. Destabilizing evolutionary and eco-evolutionary feedbacks drive empirical eco-evolutionary cycles. *Proceedings of the Royal Society B* 287: 20192298.
- De Lisle, S. P., and D. I. Bolnick. 2021. Male and female reproductive fitness costs of an immune response in natural populations. *Evolution* 75:2509–2523.
- Eckert, L., D.I. Bolnick, A. M. Derry, G. E. Haines, A.M. Heckley, A.J. Lind, C. L. Peichel, A. M. Roth, N.C. Steinel, K. Vlahiotis, J.N. Weber, A.P. Hendry, R.D.H. Barrett. 2026. Intrinsic fitness differences outweigh environmental matching in shaping introduction outcomes in nature. *BioRxiv*: <https://doi.org/10.64898/2026.02.04.699496>

- Elton, C.S. 1958. *The ecology of invasions by animals and plants*. Methuen Press.
- Fay, M. P. 2010. Two-sided exact tests and matching confidence intervals for discrete data. *R Journal* 2:53–58.
- Feis, M.E., M. A. Goedknecht, D.W. Thielges, C. Buschbaum, and K.M. Wegner. 2016. Biological invasions and host-parasite coevolution: different coevolutionary trajectories along separate parasite invasion fronts. *Zoology*. 119:366-374
- Flanagan, B.A., A. Padhiar, F. Peng, S. Quraishi, A.K. Roth-Monzón, F. Gilani, L. Simonse, M.F. Maciejewski, N. Reid, M. Malinsky, A.K. Hund, and D.I. Bolnick. 2025. Rapid genome-wide introgression reveals fitness advantage of immigrant genotypes. *BioRxiv preprint* <https://doi.org/10.1101/2025.08.27.672692>
- Fleischer, S. R., D. I. Bolnick, and S. J. Schreiber. 2021. Sick of eating: Eco-evo-immuno dynamics of predators and their trophically acquired parasites. *Evolution* 75:2842–2856.
- Fuess, L. E., J. N. Weber, S. den Haan, N. C. Steinel, K. C. Shim, and D. I. Bolnick. 2021. Between-population differences in constitutive and infection-induced gene expression in threespine stickleback. *Molecular Ecology* 30:6791–6805.
- Fuess, L.E. A.K. Hund, M.K. Kenney, M. F. Maciejewski, J.M. Marini, and D.I. Bolnick. 2025. Changes in gene regulation are associated with the evolution of resistance to a novel parasite. *BioRxiv*. doi:10.1101/2025/08/13/670117
- Fumagalli, M., M. Sironi, U. Pozzoli, A. Ferrer-Admettla, L. Pattini, and R. Nielsen. 2011. Signatures of environmental genetic adaptation pinpoint pathogens as the main selective pressure through human evolution. *PLoS Genetics* 7:e1002355.
- Grafen, A. 2015. Biological fitness and the Price Equation in class-structured populations. *Journal of Theoretical Biology* 373:62-72
- Gross, I. P., A. E. Wilson, and M. E. Wolak. 2024. The fitness consequences of wildlife conservation translocations: a meta-analysis. *Biological Reviews* 99:348–371.
- Haines, G. E., L. Moisan, A. M. Derry, and A. P. Hendry. 2023. Dimensionality and modularity of adaptive variation: divergence in threespine stickleback from diverse environments. *The American Naturalist* 201:175–199.
- Hanski, I. 1998. Metapopulation dynamics. *Nature* 396:41–49.

- Heins, D.C., D.M. Eidam, and J.A. Baker. 2016. Timing of infections in the threespine stickleback (*Gasterosteus aculeatus*) by *Schistocephalus solidus* in Alaska. *Journal of Parasitology* 102:286-289.
- Henderson, N. C., F. Rieder, and T. A. Wynn. 2020. Fibrosis: from mechanisms to medicines. *Nature* 587:555–566.
- Hendry, A. P. 2017. *Eco-evolutionary dynamics*. Princeton University Press, Princeton, NJ.
- Hendry, A. P., R. D. H. Barrett, A. M. Bell, M. A. Bell, D. I. Bolnick, K. M. Gotanda, G. E. Haines, et al. 2024. Design of eco-evolutionary experiments for restoration projects: opportunities and constraints revealed by stickleback introductions. *Ecology and Evolution* 14:e11503.
- Hund, A. K., L. E. Fuess, M. L. Kenney, M. F. Maciejewski, J. M. Marini, K. C. Shim, and D. I. Bolnick. 2022. Population-level variation in parasite resistance due to differences in immune initiation and rate of response. *Evolution Letters* 6:162–177.
- Keane, R.M., and M.J. Crawley. 2002. Exotic plant invasions and the enemy release hypothesis. *Trends in Ecology & Evolution* 17:164-170.
- Kelly, D.W., R.A. Paterson, C.R. Townsend, R. Poulin, and D.M. Tompkins. 2009. Parasite spillback: a neglected concept in invasion ecology? *Ecology* 90:2047-2056.
- Kilsdonk, L. J., and L. De Meester. 2024. Transient eco-evolutionary dynamics and the window of opportunity for establishment of immigrants. *American Naturalist* 198:E95–E110.
- Koskella, B. 2018. Resistance gained, resistance lost: an explanation for host-parasite coexistence. *PLoS Biology* 16:3000013
- Lavin, P., and J. McPhail. 1986. Adaptive divergence of trophic phenotype among freshwater populations of the threespine stickleback (*Gasterosteus aculeatus*). *Canadian Journal of Fisheries and Aquatic Sciences* 43:2455–2463.
- Lenz, T. L., C. Eizaguirre, B. Rotter, M. Kalbe, and M. Milinski. 2013. Exploring local immunological adaptation of two stickleback ecotypes by experimental infection and transcriptome-wide digital gene expression analysis. *Molecular Ecology* 22:774–786.
- Lion, S. 2018. From the Price equation to the selection gradient in class-structured populations: a quasi-equilibrium route. *Journal of Theoretical Biology* 447:178-189.
- Liu, H., and P. Stiling. 2006. Testing the enemy release hypothesis: a review and meta-analysis. *Biological Invasions* 8:1535–1545.

- Lochmiller, R.L., and C. Deerenberg. 2000. Trade-offs in evolutionary immunology: just what is the cost of immunity? *Oikos* 88:87-98.
- MacColl, A. D. C. 2009. Parasite burdens differ between sympatric three-spined stickleback species. *Ecography* 32:153–160.
- Martin, L. B., H. J. Kilvitis, A. J. Brace, L. Cooper, M. F. Haussmann, A. Mutati, V. Fasanello, et al. 2017. Costs of immunity and their role in the range expansion of the house sparrow in Kenya. *Journal of Experimental Biology* jeb.154716.
- Marzal, A., R. E. Ricklefs, G. Valkiūnas, T. Albayrak, E. Arriero, C. Bonneaud, G. A. Czirják, et al. 2011. Diversity, loss, and gain of malaria parasites in a globally invasive bird. *PLoS ONE* 6:e21905.
- Matthews, B., K. B. Marchinko, D. I. Bolnick, and A. Mazumder. 2010. Specialization of trophic position and habitat use by sticklebacks in an adaptive radiation. *Ecology* 91:1025–1034.
- Matthews, D. G., M. F. Maciejewski, G. A. Wong, G. V. Lauder, and D. I. Bolnick. 2023. Locomotor effects of a fibrosis-based immune response in stickleback fish. *Journal of Experimental Biology* 226:jeb246684.
- McElreath, R. 2016. *Statistical Rethinking*. CRC Press, Boca Raton, FL.
- Olden, J. D., M. J. Kennard, J. J. Wawler, and N. L. Poff. 2011. Challenges and opportunities in implementing managed relocation for conservation of freshwater species. *Conservation Biology* 25:40–47.
- Parmesan, C., N. Ryrholm, C. Stefanescu, J. K. Hill, C. D. Thomas, H. Descimon, B. Huntley, et al. 1999. Poleward shifts in geographical ranges of butterfly species associated with regional warming. *Nature* 399:579–583.
- Pelletier, F., T. Clutton-Brock, J. Pemberton, S. Tuljapurkar, and T. Coulson. 2007. The evolutionary demography of ecological change: linking trait variation and population growth. *Science* 315:1571–1574.
- Pelletier, F., D. Garant, and A. P. Hendry. 2009. Eco-evolutionary dynamics. *Philosophical Transactions of the Royal Society B* 364:1483–1489.
- R. Development Core Team. 2022. *R: a language and environment for statistical computing*. R Foundation for Statistical Computing.

- Sasser, K. T., S. P. De Lisle, K. A. Thompson, J. A. W. Stecyk, D. I. Bolnick, and J. N. Weber. In review. Metabolic, performance, and fecundity consequences of peritoneal fibrosis in threespine stickleback. *Functional Ecology*.
- Scharsack, J., M. Kalbe, R. Derner, J. Kurtz, and M. Milinski. 2004. Modulation of granulocyte responses in three-spined sticklebacks *Gasterosteus aculeatus* infected with the tapeworm *Schistocephalus solidus*. *Diseases of Aquatic Organisms* 59:141–150.
- Scharsack, J. P., and M. Kalbe. 2014. Differences in susceptibility and immune responses of three-spined sticklebacks (*Gasterosteus aculeatus*) from lake and river ecotypes to sequential infections with the eye fluke *Diplostomum pseudospathaceum*. *Parasites and Vectors* 7:109.
- Scharsack, J. P., M. Kalbe, C. Harrod, and G. Rauch. 2007. Habitat-specific adaptation of immune responses of stickleback (*Gasterosteus aculeatus*) lake and river ecotypes. *Proceedings of the Royal Society B* 274:1523–1532.
- Schatz, A. M., and A. W. Park. 2023. Patterns of host–parasite coinvasion promote enemy release and specialist parasite spillover. *Journal of Animal Ecology* 92:1029–1041.
- Schluter, D. 1993. Adaptive radiation in sticklebacks: Size, shape, and habitat use efficiency. *Ecology* 74:699–709.
- Schluter, D., and J. D. McPhail. 1992. Ecological character displacement and speciation in sticklebacks. *American Naturalist* 140:85–108.
- Seppälä, O. 2015. Natural selection on quantitative immune defence traits: a comparison between theory and data. *Journal of Evolutionary Biology* 28:1–9.
- Shaw, C.L., R. Bilich, and M.A. Duffy. 2024. A common multi-host parasite shows genetic structuring at the host species and population levels. *Parasitology* 151:557–566.
- Snowberg, L. K., K. M. Hendrix, and D. I. Bolnick. 2015. Covarying variances: more morphologically variable populations also exhibit more diet variation. *Oecologia* 178:89–101.
- Sriramulu, P., D. Schluter, and D. I. Bolnick. 2025. Dynamics of infection and immunity over 50 years in an experimentally founded population of stickleback. *Evolution Letters* 9:383–391
- Stewart, A., J. Jackson, I. Barber, C. Eizaguirre, R. Paterson, P. van West, C. Williams, et al. 2017. Hook, Line and Infection. Pages 39–109 in *Advances in Parasitology* (Vol. 98). Elsevier.
- Stutz, W. E., O. L. Lau, and D. I. Bolnick. 2014. Contrasting patterns of phenotype-dependent parasitism within and among populations of threespine stickleback. *The American Naturalist* 183:810–825.

- Taylor, P.D. 1990. Allele-frequency change in a class-structured population. *American Naturalist* 135:95-106.
- Torchin, M. E., K. D. Lafferty, A. P. Dobson, V. J. McKenzie, and A. M. Kuris. 2003. Introduced species and their missing parasites. *Nature* 421:628–630.
- Trewby, I. D., G. J. Wilson, R. J. Delahay, N. Walker, R. Young, J. Davison, C. Cheeseman, et al. 2007. Experimental evidence of competitive release in sympatric carnivores. *Biology Letters* 4:170–172.
- Walsh, J. R., S. R. Carpenter, and M. J. Vander Zanden. 2016. Invasive species triggers a massive loss of ecosystem services through a trophic cascade. *Proceedings of the National Academy of Sciences of the USA* 113:4081–4085.
- Wang, A., and D. I. Bolnick. 2025. Among-population proteomic differences in *Schistocephalus solidus* based on excretory/secretory and total body protein predictions. *Parasites and Vectors*. 18:180.
- Weber, J. N., M. Kalbe, K. C. Shim, N. Erin, N. Steinel, and D. I. Bolnick. 2017a. Resist globally, infect locally: a trans-continental test of coevolution and local adaptation by stickleback and their cestode parasite. *American Naturalist* 189:43-57.
- Weber, J. N., N. C. Steinel, F. Peng, K. C. Shim, B. K. Lohman, L. E. Fuess, S. Subramanian, et al. 2022. Evolutionary gain and loss of a pathological immune response to parasitism. *Science* 377:1206–1211.
- Weber, J. N., N. C. Steinel, K. C. Shim, and D. I. Bolnick. 2017b. Recent evolution of extreme cestode growth suppression by a vertebrate host. *Proceedings of the National Academy of Sciences of the USA* 114:6575–6580.
- White, T. A., and S.E. Perkins 2012. The ecoimmunology of invasive species. *Functional Ecology* 26:1313:1323.
- Wilber, M. Q., J. A. DeMarchi, C. J. Briggs, and S. Streipert. 2024. Rapid evolution of resistance and tolerance leads to variable host recoveries following disease-induced declines. *American Naturalist* 203:535-550.
- Willacker, J. J., F. A. Von Hippel, P. R. Wilton, and K. M. Walton. 2010. Classification of threespine stickleback along the benthic-limnetic axis. *Biological Journal of the Linnean Society* 101:595–608.
- Yamamichi, M. 2022. How does genetic architecture affect eco-evolutionary dynamics? A theoretical perspective. *Philosophical Transactions of the Royal Society B* 377:20200504.

Figure Legends

Figure 1. The experimental design and information about genetic, ecological, and immunological differences among the source lakes. **(A)** We identified eight lakes with native stickleback (map in supplementary fig. S2). We display different stickleback icons to distinguish the ecotypes in these lakes (benthic: deep-bodied fish in light green lakes; limnetic: fusiform fish in light blue lakes), and represent variation in lake size. In 2019 we collected fish from four morphologically benthic populations, or four morphologically limnetic populations and factorially introduced these into four smaller recipient lakes (dark green lake icons) and four larger recipient lakes (dark blue icons). A ninth lake received a mix of both pools. The 2019 G Lake introduction failed (red X) and was reintroduced successfully in 2022 with a mixed pool. Created in BioRender. Bolnick, D. (2026) <https://BioRender.com/5ixjuj>. **(B)** A neighbor joining phylogenetic tree showing genetic divergence between source lake populations, rooted by two marine anadromous populations from Sayward Estuary (British Columbia) and Rabbit Slough (Alaska). Redrawn from Weber et al. 2022. **(C)** Source lakes differed in *Schistocephalus solidus* prevalence (2019-2024). The x axis is on a log scale. **(D)** Fibrosis severity differed among source lakes (means with standard errors), colored by population ecotype (light blue for limnetic, light green for benthic).

Alt Text: A multi-paneled figure. Panel A shows a schematic diagram of the experimental design with eight benthic and limnetic source lakes being used to found populations in nine benthic or limnetic recipient lakes. Panel B shows a phylogenetic tree confirming there is genetic divergence among source lakes. Panel C and D show that *S. solidus* infection rates and fibrosis differ between source lakes, with dots representing point estimates and standard error bars.

Figure 2. Peritoneal fibrosis in stickleback is induced by *S. solidus* infection, but this response varies heritably among source populations. **(A)** Fibrosis is more severe in larger source lakes. Data points represent lake means over all sampled years, color coded by source population ecotype (green benthic, blue limnetic), with standard error bars. Points are scaled relative to log lake area. **(B)** Fibrosis is higher

in uninfected than in infected individuals within most source lakes. Each lake is one point with standard error bars, the diagonal line indicates equal fibrosis in infected and uninfected fish. (C) Fibrosis varies among source lake populations raised in the laboratory and experimentally fed *S. solidus*-infected copepods to create controlled exposures. We plot fibrosis means of exposed fish from different lakes (with standard error bars). Lakes are ordered from small (left) to large (right) with point sizes scaled to lake area. A low-fibrosis marine population (Kenai Estuary, black point) is included to represent an ancestral character state. Long Lake was excluded because we failed to obtain sufficient numbers of breeding fish to stock a lab population for this experiment.

Alt Text: A multi-paneled figure. Panel A shows fibrosis (y axis) covarying positively with lake size (x axis), with one point for each lake representing the estimate with standard error bars. Panel B shows the mean fibrosis for infected fish within each lake (y axis) and mean fibrosis for uninfected fish within each lake (x axis). The points fall above a diagonal line, indicating higher fibrosis in infected individuals. Panel C shows that mean fibrosis score differs among lakes, in lab-raised fish exposed to tapeworm infections, with one point per lake, with standard error bars.

Figure 3. Ecological release in the newly founded stickleback populations. On average, recipient lake populations (blue) exhibit persistently lower *S. solidus* infection rates compared to the source lake populations (red) from which they were derived. The reduced infection rate in recipient lakes is consistent with the ‘enemy release hypothesis’. Year effect (treated as a factor rather than linear trend), $F_{3,54} = 1.2$, $P = 0.311$; Source/Recipient effect $F_{1,54} = 10.7$, $P = 0.0019$; Year \times source/recipient interaction effect $F_{3,54} = 1.7$, $P = 0.161$.

Alt Text: A single panel figure with tapeworm prevalence (y axis) as a function of year (x axis) with different colored points and linear trendlines for source and recipient lakes. The line for recipient lakes is consistently lower than for source lakes. A confidence band around the trend lines is shown for each group of lakes.

Figure 4. Temporal dynamics of *S. solidus* infection prevalence and fibrosis severity in source and recipient lakes. Lakes are color coded by source lake fish ecotypes (light green for benthic and light blue for limnetic), or ecotype pools used to found populations (dark green and dark blue; brown for Loon Lake which received both founder pools). In panels B and D, symbol shapes distinguish recipient lake habitat type. **(A)** Infection rates varied among source lakes with a relatively weak effect of time. **(B)** Infection rates in experimentally founded populations exhibit a much stronger lake×year interaction. **(C)** Fibrosis varied substantially among source lakes with comparatively weak but still significant effects of year, and a lake×year interaction. **(D)** Fibrosis severity diverged among recipient lake populations with a substantially larger effect of lake×year interactions, as well as differences between lake ecotypes, and ancestry pools. Note: source lakes were not sampled in 2020 or 2025, and the 2019 recipient lake values are based on the mean of the source lake pools used to found the new populations.

Alt Text: A multi-paneled figure showing variation in log *S. solidus* infection rates (panels A and B, top row) as a function of year, with lines drawn for each source lake (panel A) or each recipient lake (panel B). The bottom row shows variation in fibrosis over time, with lines for each source lake (panel C) and recipient lake (panel D). Lakes are color coded by ecotype (A,C) or lake size (B, D).

Figure 5. In the recipient lakes, temporal changes in *S. solidus* prevalence are linked to changes in their hosts' fibrosis response. **(A)** Initially, fibrosis tended to be higher in recipient lakes with higher infection prevalence, though the relationship weakened then reversed in later years. The temporal change in this slope is shown in Fig. S5. Each regression line with shaded confidence interval (and point shape) is for a separate year. Thick solid lines are statistically significant ($P < 0.05$), thin solid lines marginally so ($P < 0.1$), and dashed lines non-significant. **(B)** Recipient lakes with more fibrosis in a given year exhibited a larger decrease in tapeworm prevalence the following year. Each between-year comparison is represented by a different-colored trendline with shaded confidence interval and different color/shape points. A horizontal line is provided to indicate zero change. **(C)** Recipient lakes with more *S. solidus* in a given year, exhibited a decline in tapeworm prevalence the following year, indicating a negative temporal auto-

correlation. Each regression line (with 1 s.e. confidence intervals) is a between-year comparison. The grey area denotes unfeasible combinations. See supplementary fig. S6 for an equivalent analysis within the source lakes.

Alt Text: A multi-paneled figure. Panel A represents the relationship between fibrosis and *S.solidus* prevalence in the recipient lakes, with each year represented as a separate trend line and points (with confidence band around the trend line). Panel B represents how fibrosis (x axis) in one year, affects the subsequent change in *S.solidus* prevalence (y axis), with a separate trend line and colored points for each between-year interval. Panel C represents how the between-year change in *S.solidus* prevalence (y axis) depends on the previous year's *S. solidus* prevalence, with a separate colored line and points for each between-year interval.

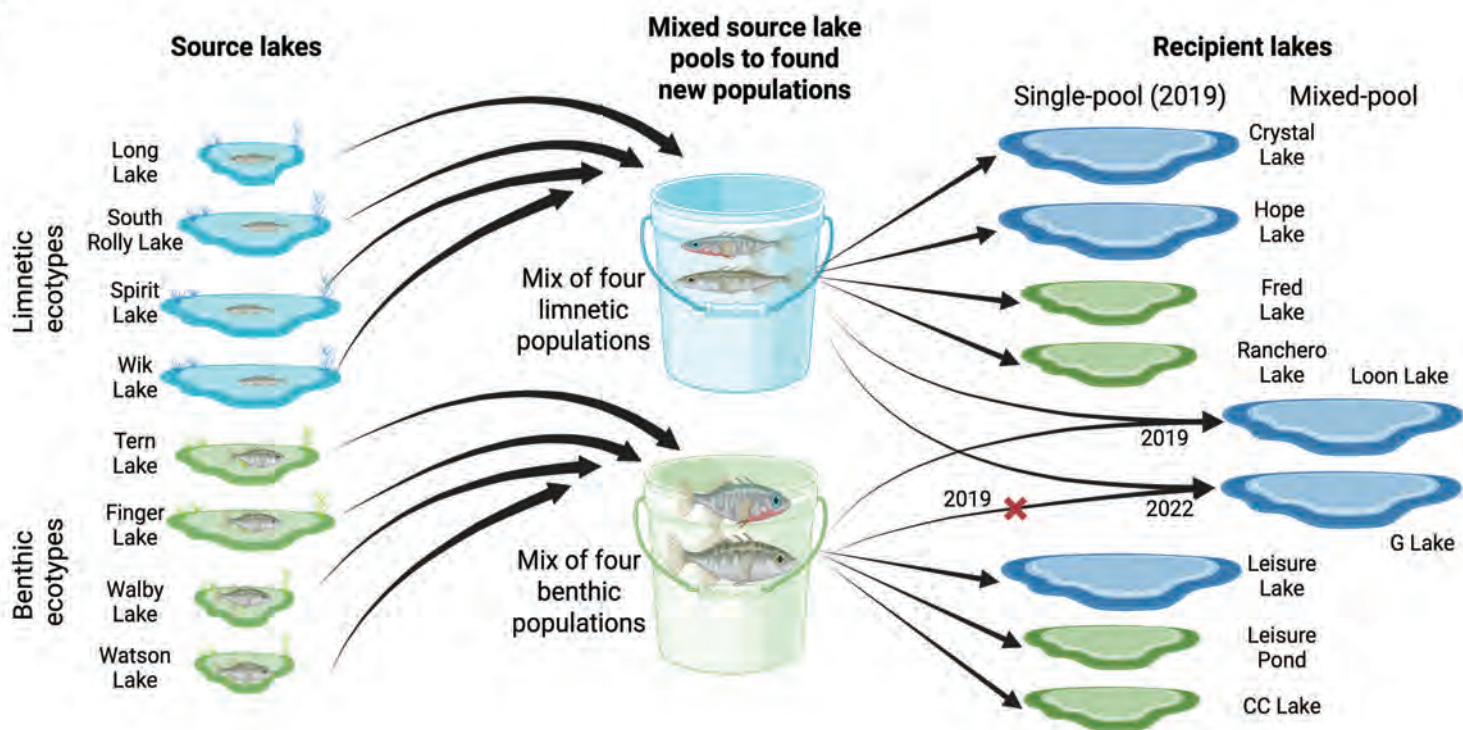
Figure 6. In the recipient lakes, temporal changes in *S. solidus* prevalence are linked to changes in their hosts' fibrosis response. **(A)** Fibrosis exhibits heritable variation within the admixed recipient lake populations: the fibrosis score of an individual depends on their source lake ancestry. Bayesian posterior effect means and 95% credibility intervals are plotted (parameters whose credibility interval excludes zero are marked with asterisks). Fish with greater proportional ancestry from Finger or Long Lake had stronger fibrosis, while Walby and South Rolly Lake ancestry reduced fibrosis. Equivalent results for infection rate are presented in supplementary fig. S8. These ancestry effect estimates from the experimental recipient lakes are positively correlated with **(B)** the severity of fibrosis in the original source lakes, and **(C)** the strength of fibrosis in lab-raised fish following cestode exposure. Note Long Lake was not used in the lab study so is not shown in (C).

Alt Text: A multi-paneled figure. Panel A represents the estimates of how ancestry affects fibrosis within the recipient lakes. Panel B shows that these estimates in wild recipient lake fish (y axis) are positively correlated with fibrosis rates in the original source lakes (x axis), with one pint per source lake. Panel C shows that these ancestry effects in the wild (y axis) is positively related to laboratory measures of fibrosis (x axis) with one point per source lake.

Figure 7. Recipient lake populations evolved between their founding in 2019 and 2021, as evidenced by changing frequencies of source lake genotypes. **(A)** In lakes that received benthic pool founders (or a mix), Walby Lake ancestry generally increased (but decreased in Loon Lake) resulting in significant variation in Walby ancestry ($F_{3,382}=40.67$, $P < 0.0001$). The zeroes are lakes that did not receive a particular ancestry. **(B)** In lakes that received limnetic pool founders (or a mix), by 2021 South Rolly ancestry varied between lakes ($F_{4,478}=5.06$, $P < 0.0001$), two lakes exhibiting significant increases in South Rolly genotypes. These changes in genotype frequency are larger than can be explained by founder effects, drift, and sampling (fig. S9). **(C, D)** Changes in Walby and South Rolly ancestry (from 2019 to 2021) are correlated with fibrosis differences among recipient lakes in 2021.

Alt Text: A multi-paneled figure. Panels A and B (top row) show that within the recipient lakes, source lake ancestry proportions change from the initial founded population to 2021, with a trend line for each recipient lake. Panels C and D show that the change in ancestry proportion (for two focal ancestry groups, Walby and South Rolly Lakes) is related to the fibrosis severity in the recipient lakes in 2021.

A



Sayward Estuary
 Rabbit Slough

B

C

D

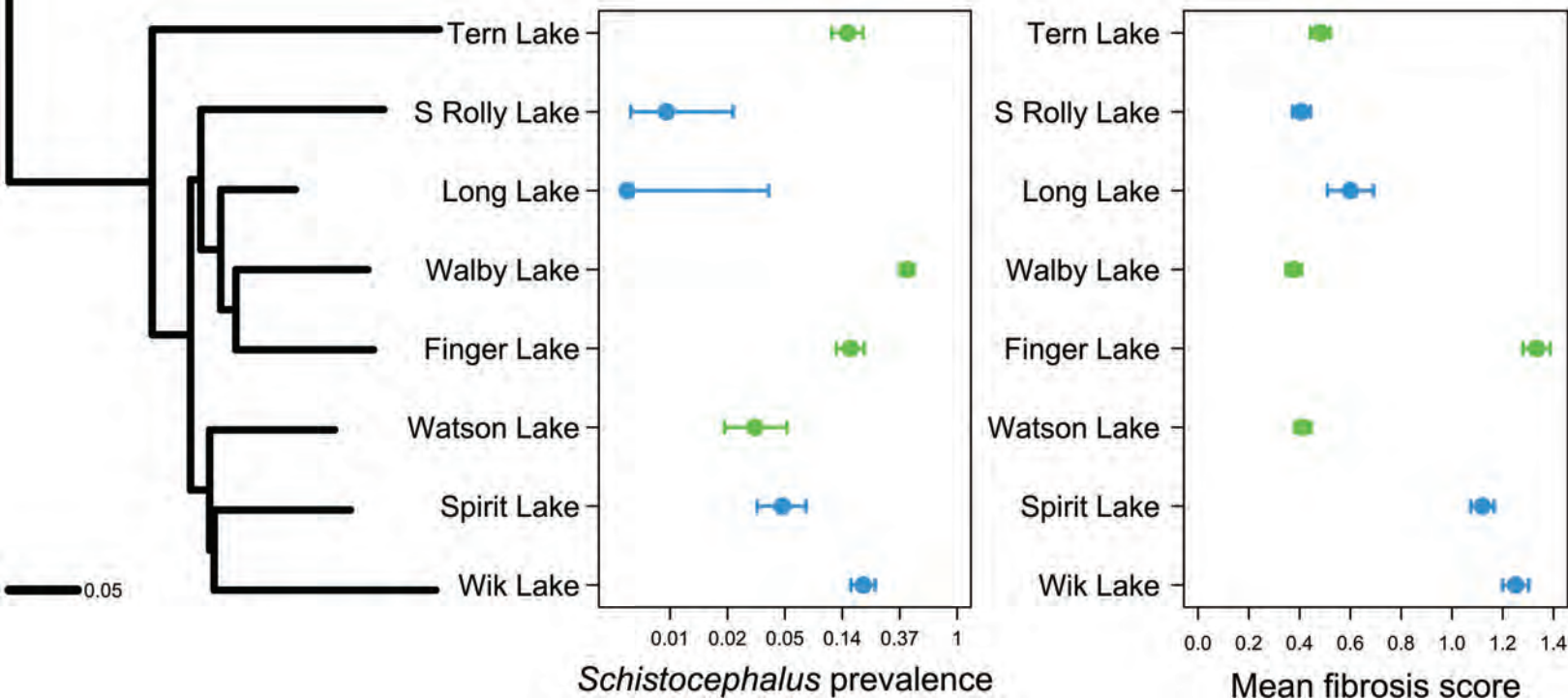


Figure 2

This is not a published article. This is an accepted manuscript, without copyediting, corrections, proofreading, or online data files, and before publication. The completed version of record is expected to be published with DOI <https://doi.org/10.1086/741682> in an upcoming issue of The American Naturalist, published by The University of Chicago Press. Copyright 2020 The University of Chicago.

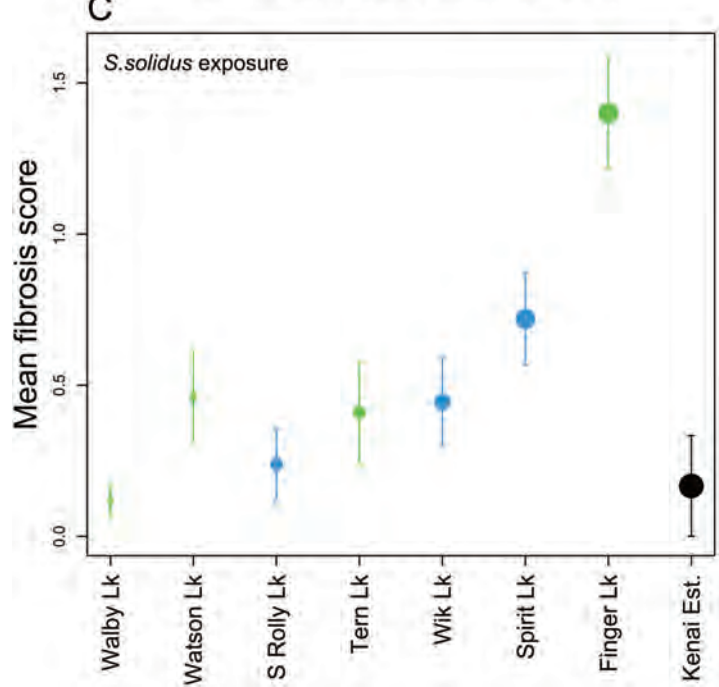
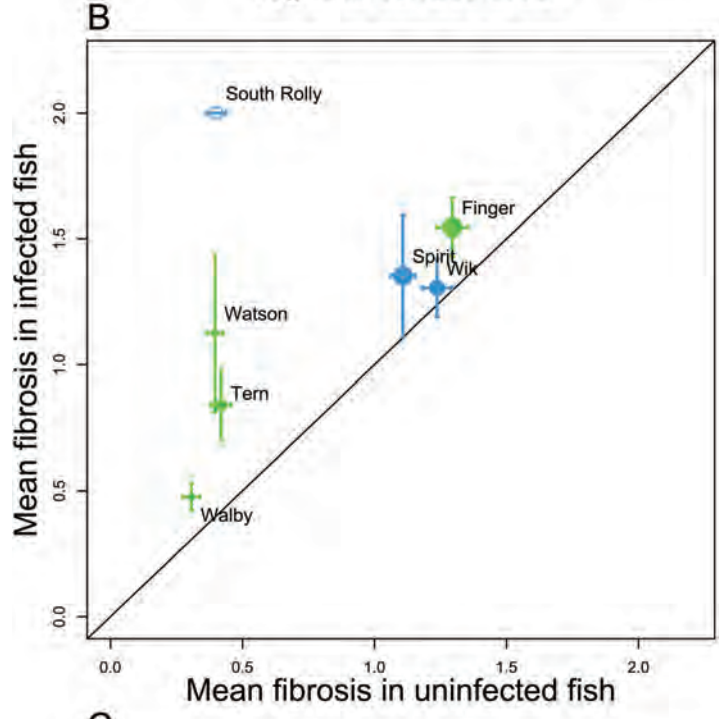
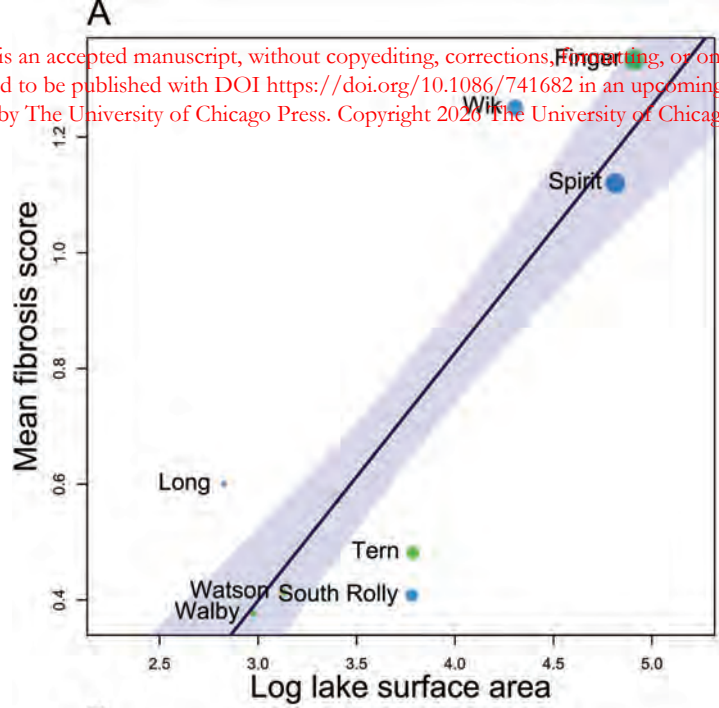


Figure 3

This is not a published article. This is an accepted manuscript, without copyediting, corrections, formatting, or online data files, and before publication. The completed version of record is expected to be published with DOI <https://doi.org/10.1086/741682> in an upcoming issue of *The American Naturalist*, published by The University of Chicago Press. Copyright 2026 The University of Chicago.

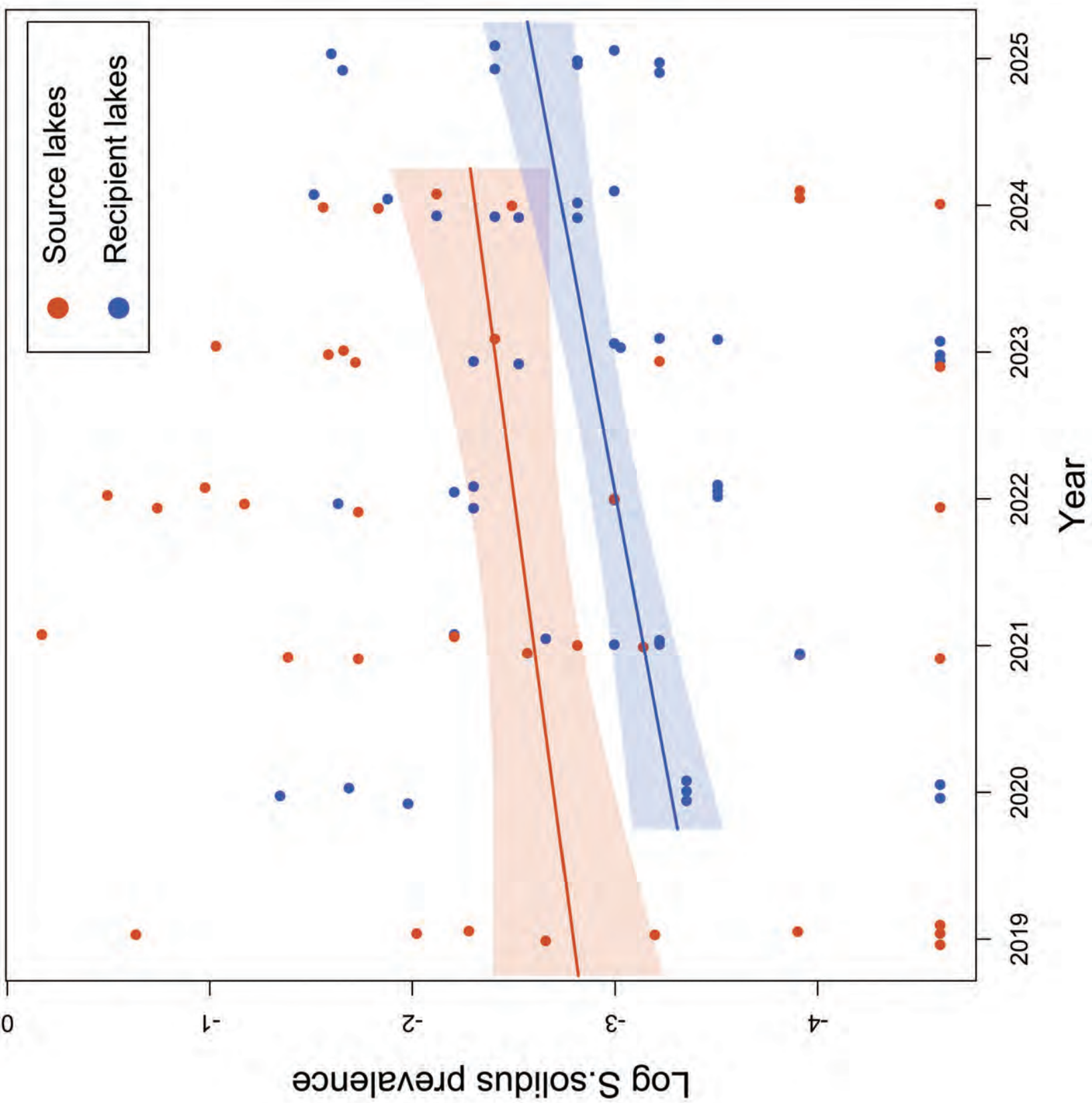


Figure 4

This is not a published article. This is an accepted manuscript, without copyediting, corrections, formatting, or online data files, and before publication. The completed version of record is expected to be published with DOI <https://doi.org/10.1086/741682> in an upcoming issue of The American Naturalist, published by The University of Chicago Press. Copyright 2026 The University of Chicago.

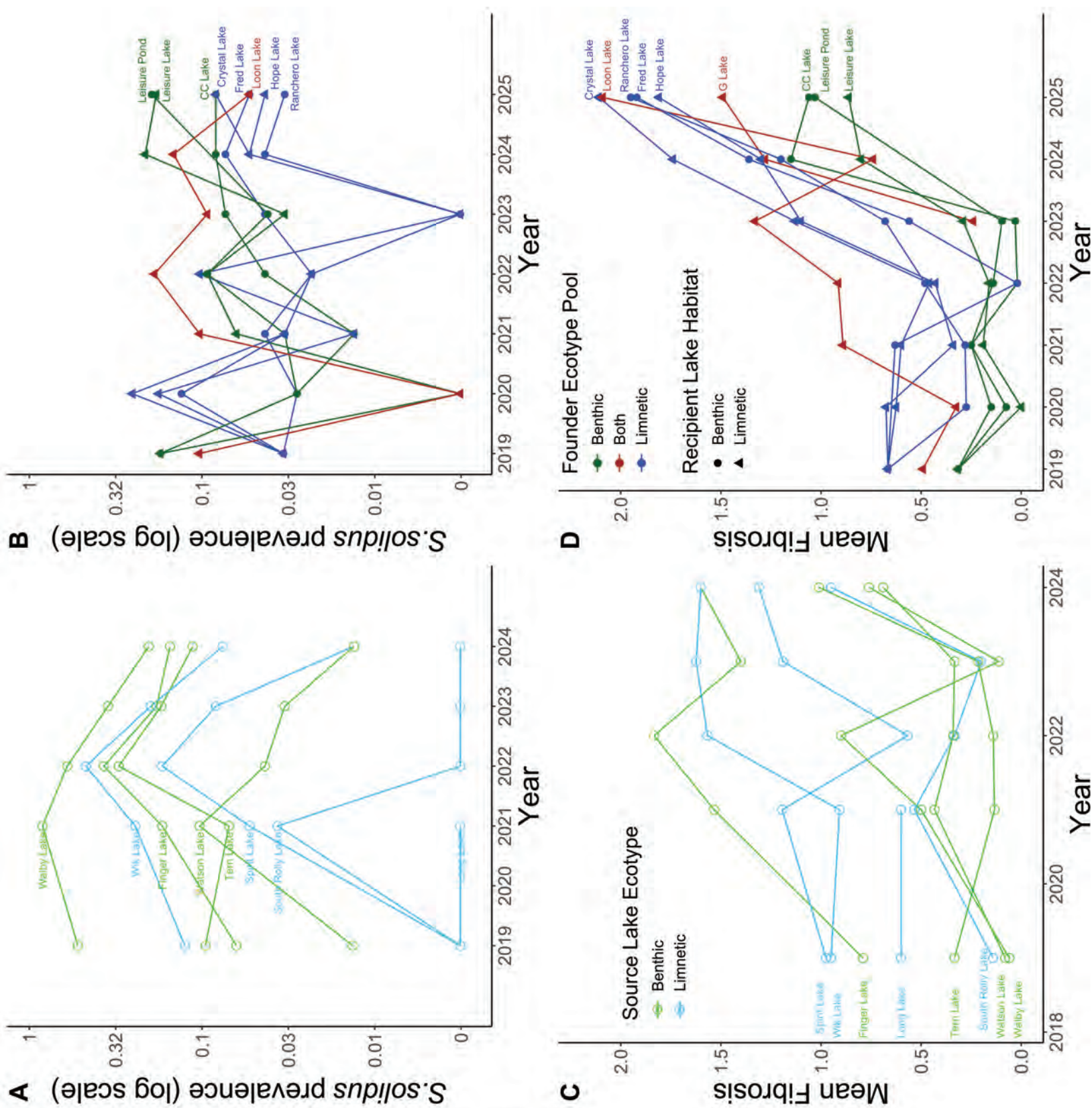


Figure 5

This is not a published article. This is an accepted manuscript, without copyediting, corrections, formatting, or online data files, and before publication. The completed version of record is expected to be published with DOI <https://doi.org/10.1086/741682> in an upcoming issue of The American Naturalist, published by The University of Chicago Press. Copyright 2026 The University of Chicago.

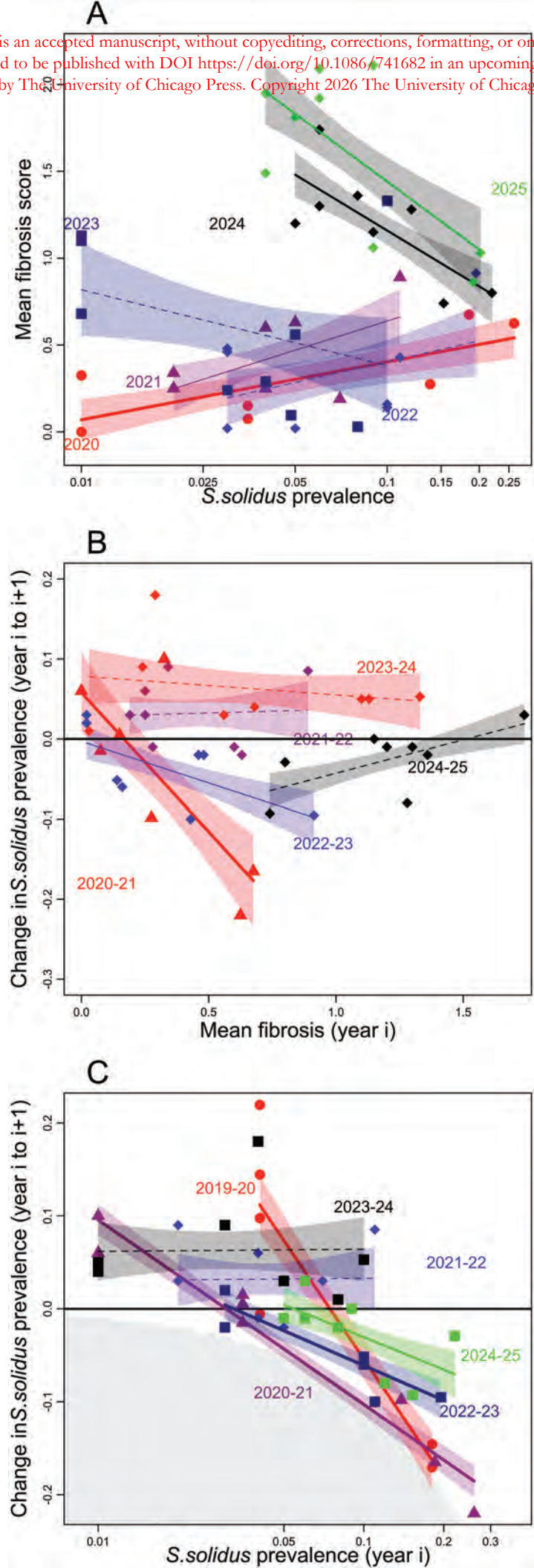
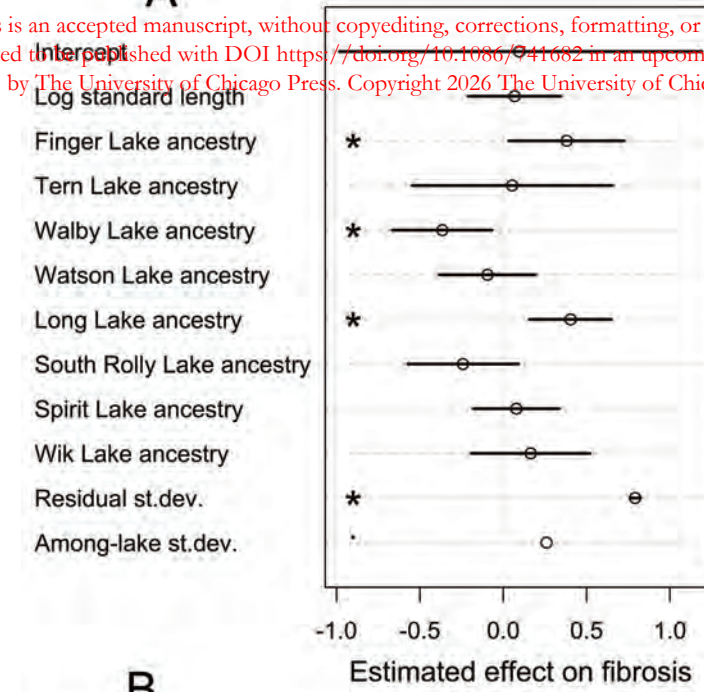
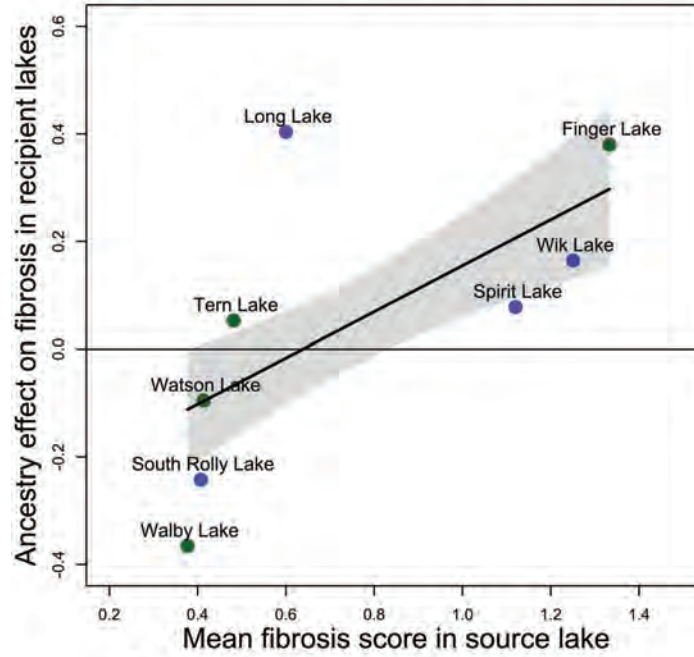


Figure 6

A



B



C

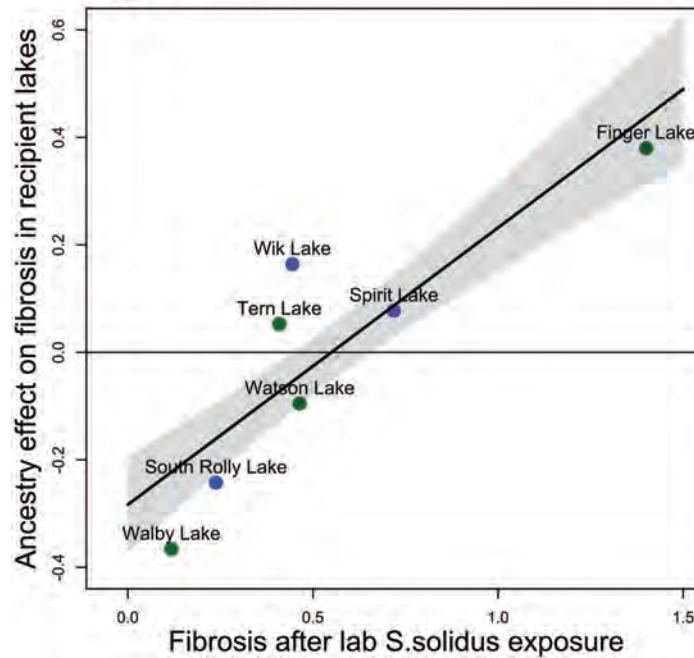
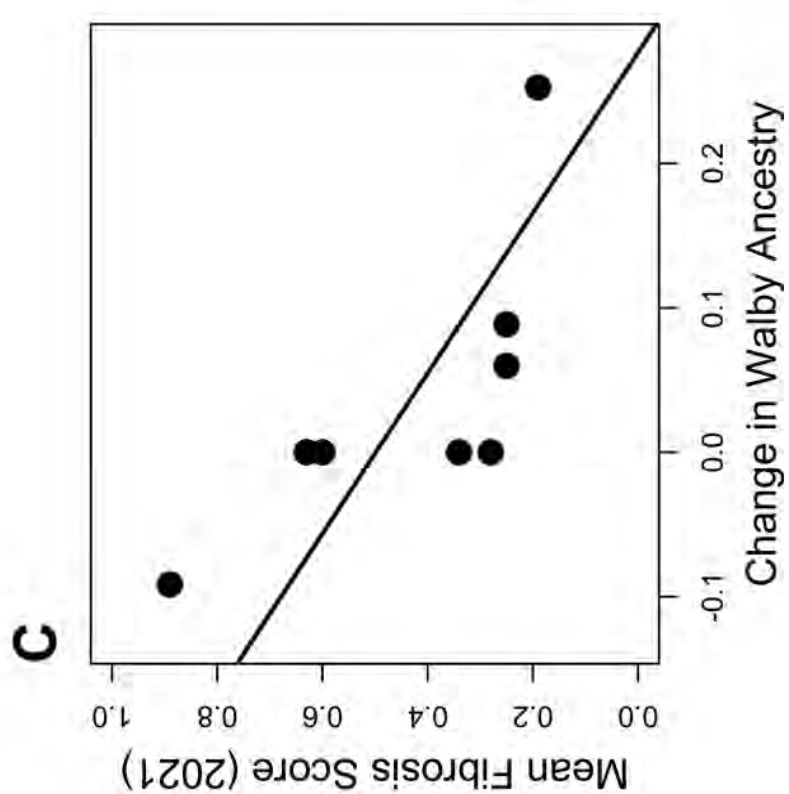
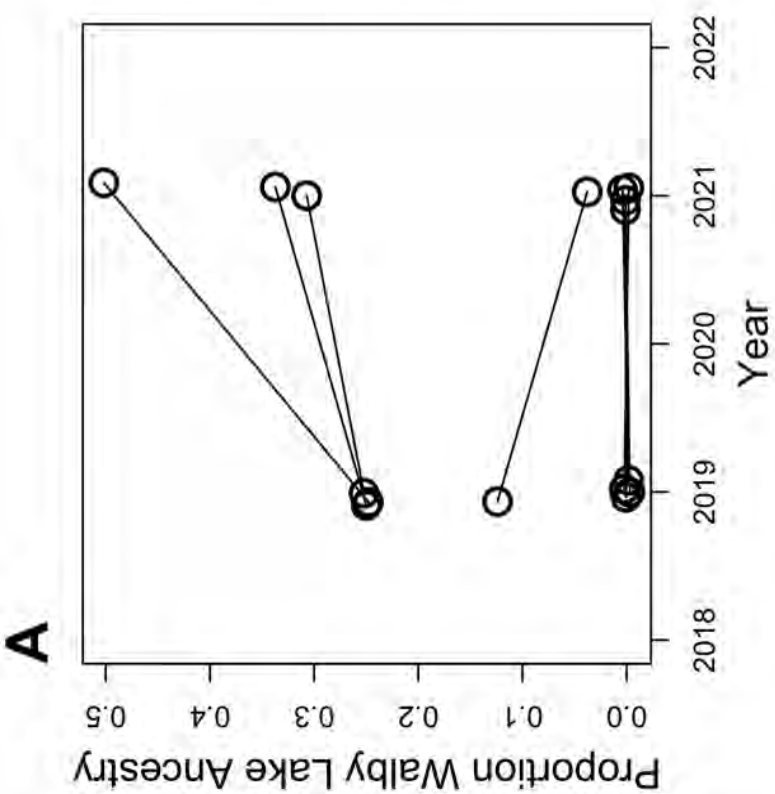
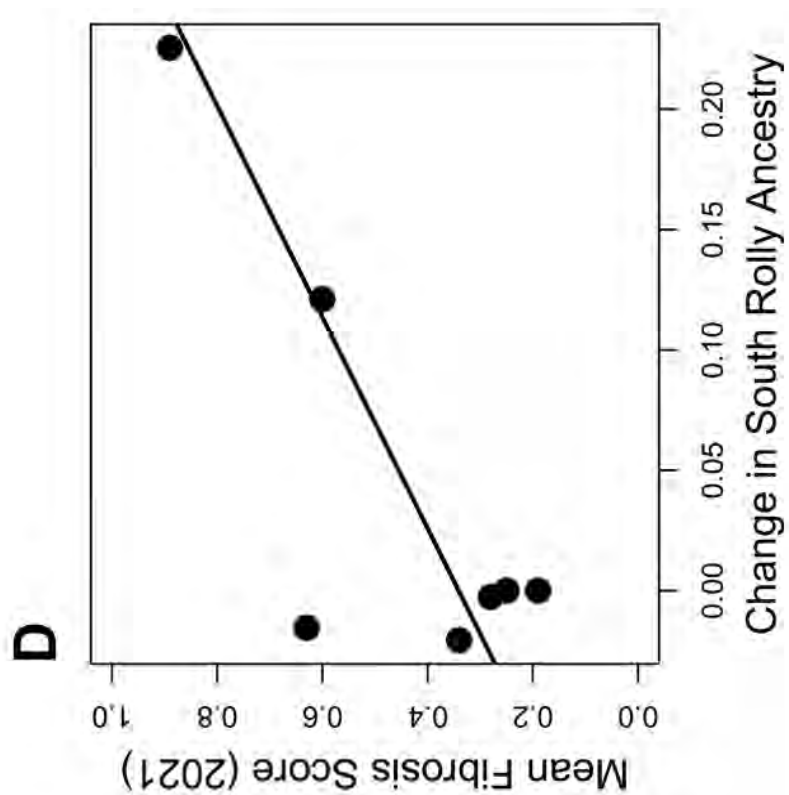
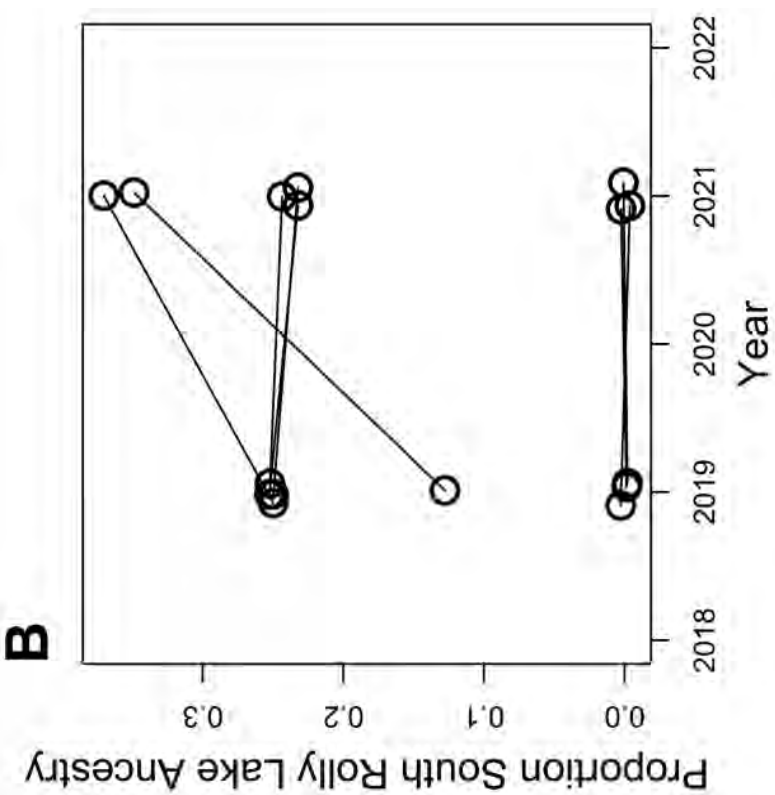


Figure 7

This is not a published article. This is an accepted manuscript, without copyediting, corrections, formatting, or online data files, and before publication. The completed version of record is expected to be published with DOI <https://doi.org/10.1086/741682> in an upcoming issue of *The American Naturalist*, published by The University of Chicago Press. Copyright 2026 The University of Chicago.



Supplementary Materials for:

Destabilized host-parasite dynamics in newly founded populations

Daniel I. Bolnick,^{1*} Lucas Eckert,² Rowan D.H. Barrett,² Emma Choi,¹ Grant Haines,^{2,3}

Andrew P. Hendry,² Emily V. Kerns,⁴ Åsa J. Lind,^{2,5} Kathryn Milligan-McClellan,⁶ Catherine L. Peichel,⁵

Kristofer Sasser,⁴ Alice R Thornton,⁷ Cole Wolf,⁴ Natalie C. Steinel,^{7,8} Jesse N. Weber^{4*}

¹ Department of Ecology and Evolutionary Biology, University of Connecticut Storrs CT, USA.

² Department of Biology, McGill University, Montreal, Quebec, Canada

³ University of Holar, Holar, Iceland

⁴ Department of Integrative Biology, University of Wisconsin, Madison, WI, USA

⁵ Division of Evolutionary Ecology, Institute of Ecology and Evolution, University of Bern, Bern, Switzerland

⁶ Department of Molecular and Cell Biology, University of Connecticut, Storrs, CT, USA

⁷ Center for Pathogen Research and Training, University of Massachusetts, Lowell, MA, USA

⁸ Department of Biology, University of Massachusetts, Lowell, USA

*Corresponding authors. Email: daniel.bolnick@uconn.edu or jnweber2@wisc.edu

The American Naturalist

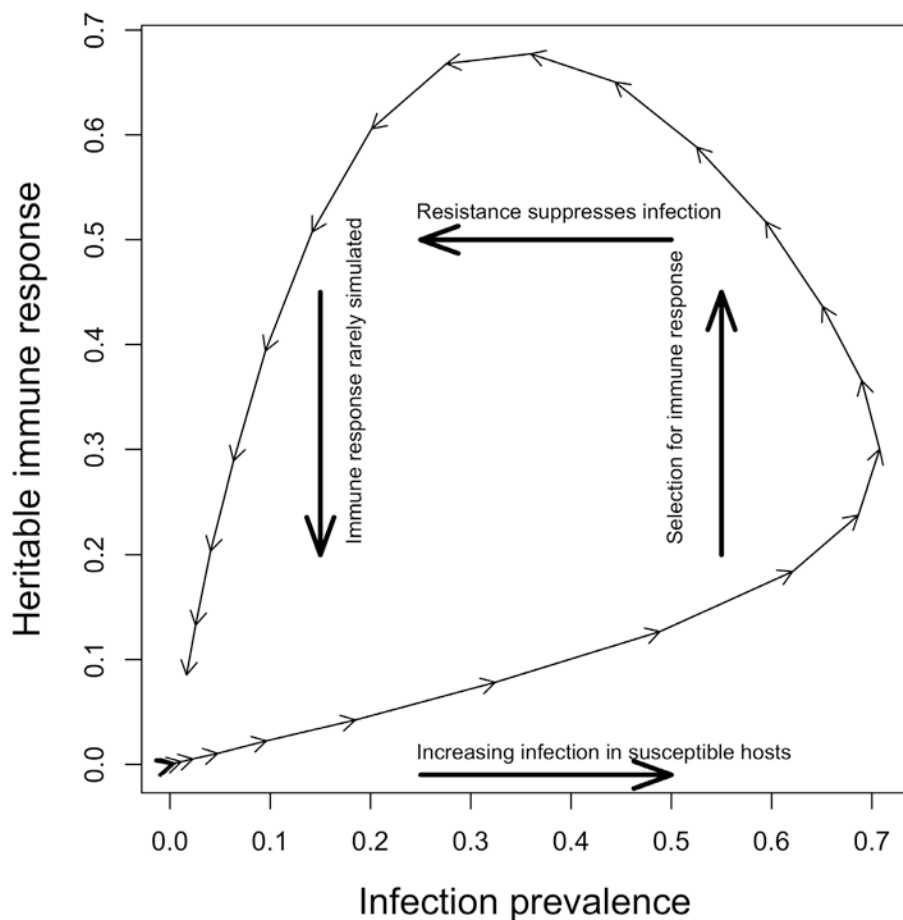
The PDF file includes:

Figs. S1 to S10

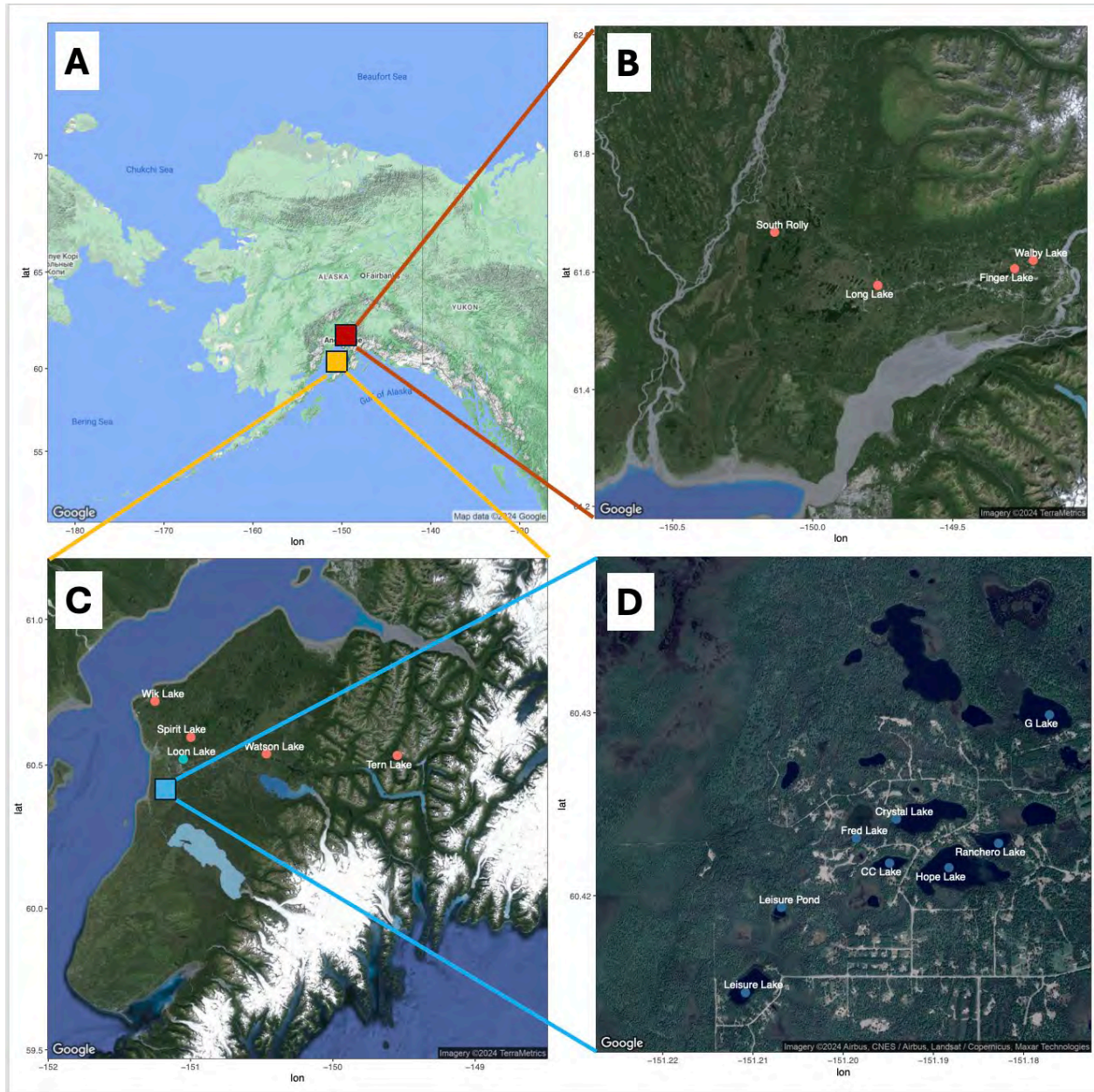
Tables S1 to S5

Supplementary Text A

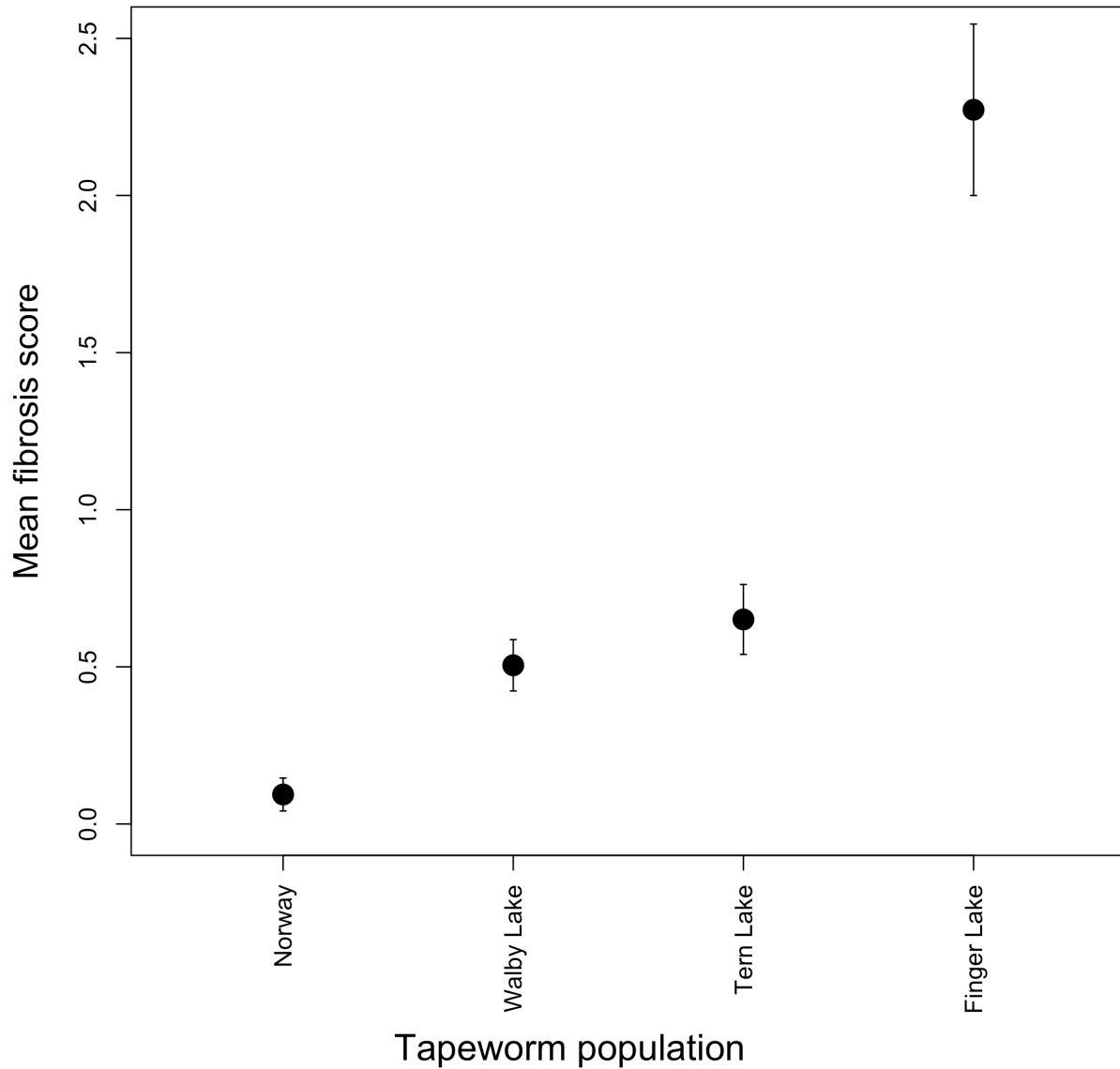
Supplementary Text B



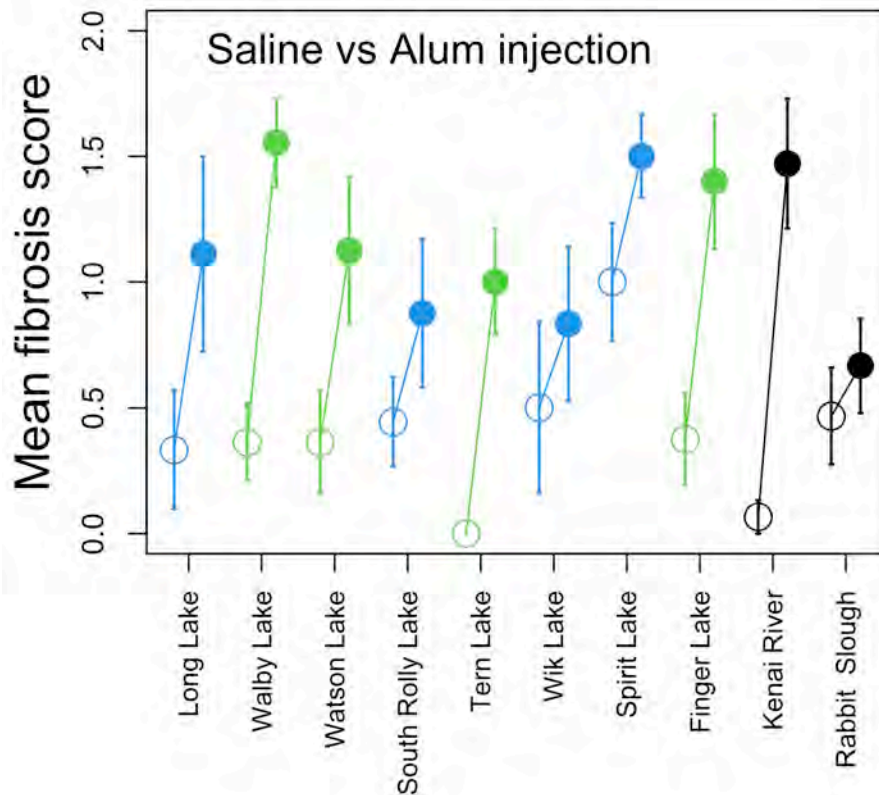
Supplementary figure S1. Numerical simulations representing eco-evolutionary dynamics of an inducible immune response to a parasite. The simulations are described in depth in Sriramulu et. al. 2025, and are not detailed here. Briefly, we begin by assuming an initially susceptible host population contains a rare allele enabling an inducible immune response to a parasite infection. The induced response is effective at suppressing parasite viability. In the initially vulnerable host population, a parasite begins to successfully infect, reproduce, and spread to new hosts. As the parasite becomes common it reduces host mean fitness, increasing selection to favor the host genotypes with the capacity for an induced immune response. As the immune genotype becomes common, the immune trait increases in intensity. This suppresses parasite abundance. As parasite abundance falls, fewer and fewer hosts are being exposed to the parasite and the inducible trait is no longer stimulated (although the genetic capacity to generate the trait persists). If there are constitutive costs to the trait, then once parasite abundance is low enough then selection may act to remove the immune trait, leading to a newly vulnerable host population. Then the cycle might resume. This model, which was designed with the stickleback system in mind, represents our expectations for stickleback-fibrosis-tapeworm eco-evolutionary dynamics.



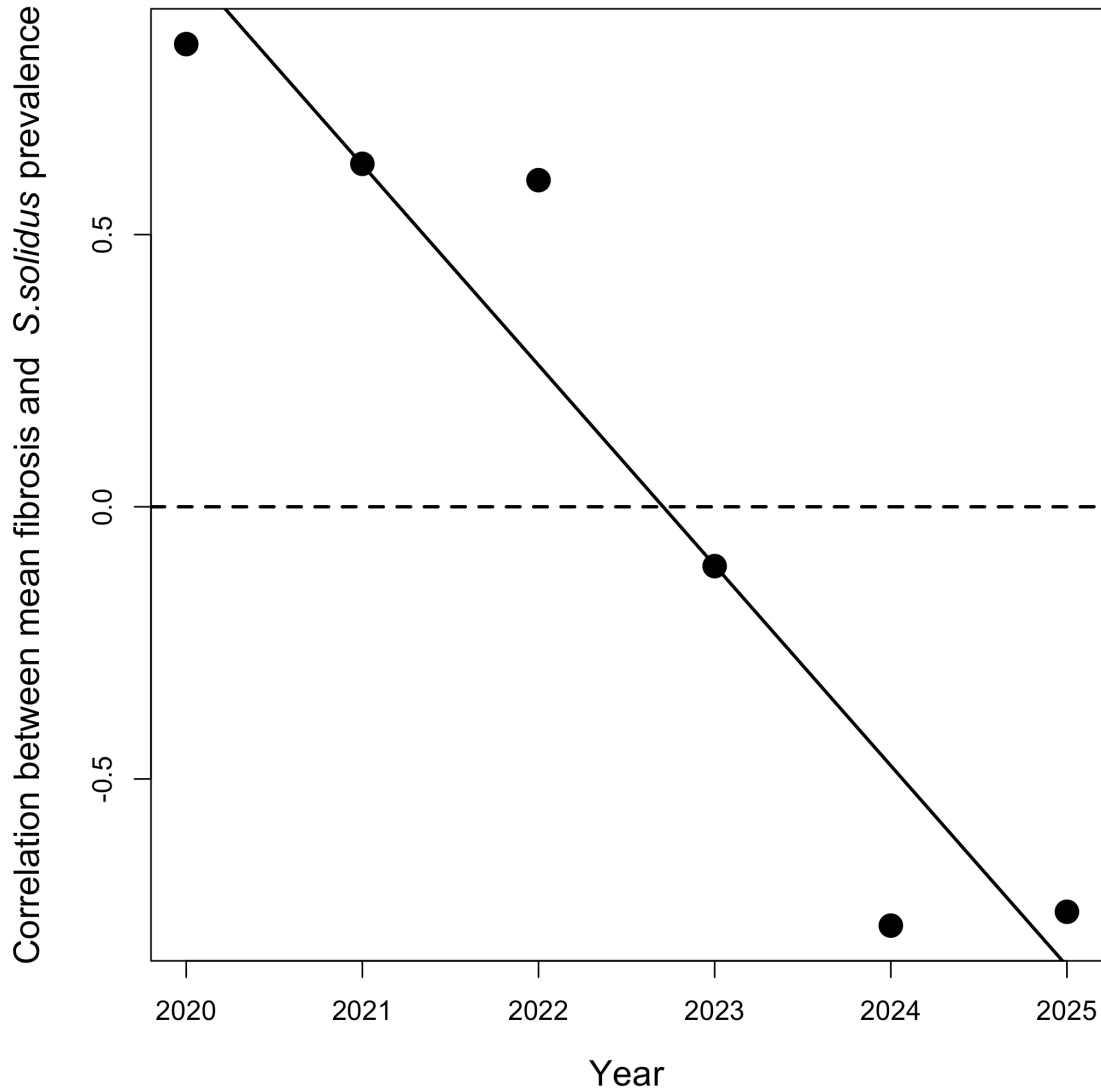
Supplementary figure S2. Map of populations used as sources of founders (red points) and fishless recipient lakes (blue points). (A) A view of Alaska showing the location of the Mat-Su Valley (red box) and Kenai Peninsula (orange box). (B) Zoom in to four source lakes in the Mat-Su regions. (C) Zoom in to the Kenai Peninsula showing the locations of four source lakes (red points) and recipient lakes (blue). (D) Zoom in to eight of the recipient lakes.



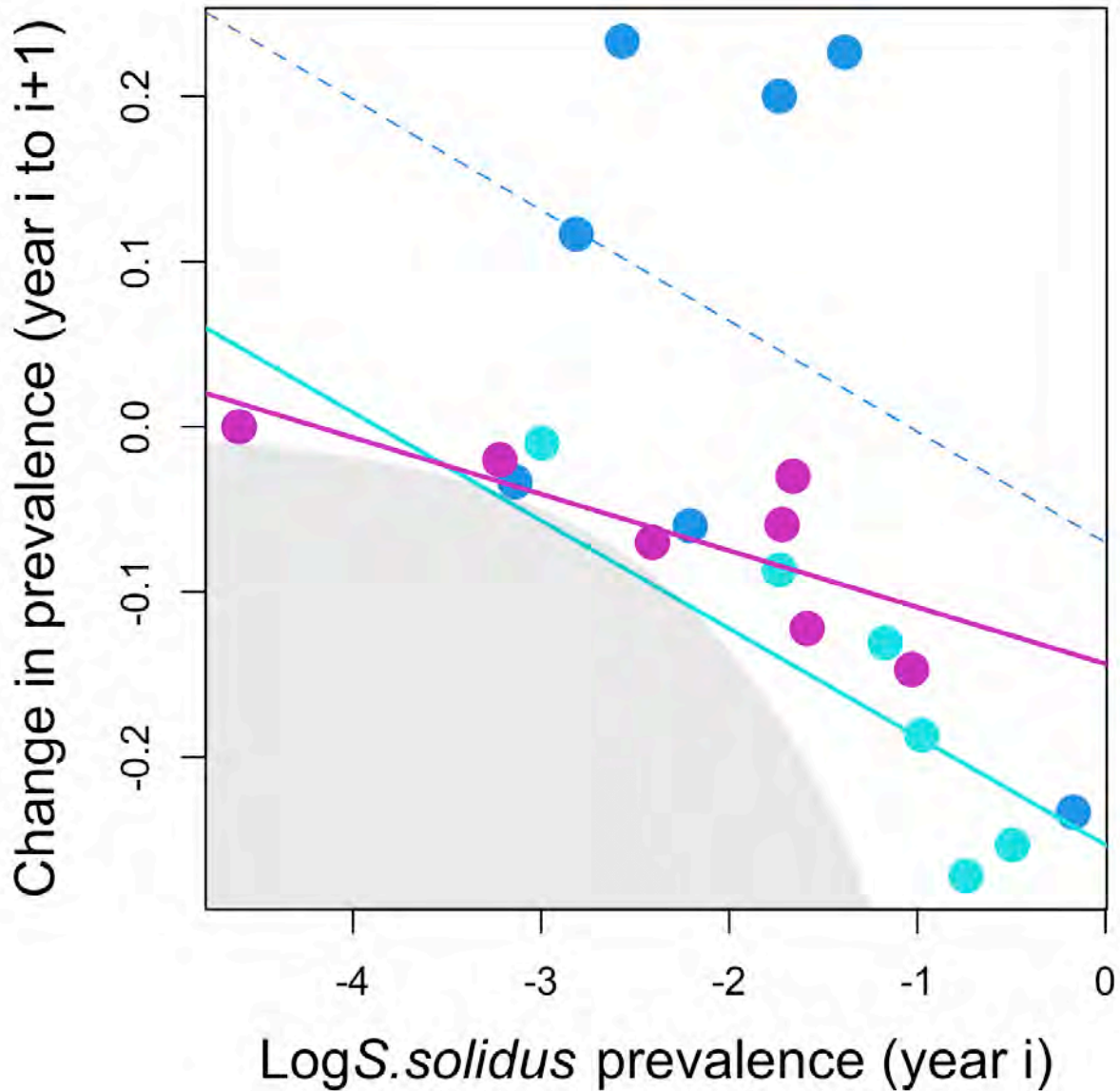
Supplementary figure S3. Tapeworm populations induce divergent fibrosis responses in lab-raised stickleback (fibrosis score was zero for all sham-exposed individuals), averaging across fish populations. Effect sizes here are least squares means after accounting for host fish genotype. Exposed fish were fed copepods containing procercoids from one of four *S. solidus* source populations. A linear model confirms that fibrosis depends on both stickleback genotype ($F_{7,196}=10.3$, $P<0.0001$, fig 2C) and tapeworm strain ($F_{3,196}=8.9$, $P<0.0001$, shown here), though there is no detectable fish by parasite genotype interaction effect ($F_{12,184}=1.2$, $P=0.2832$).



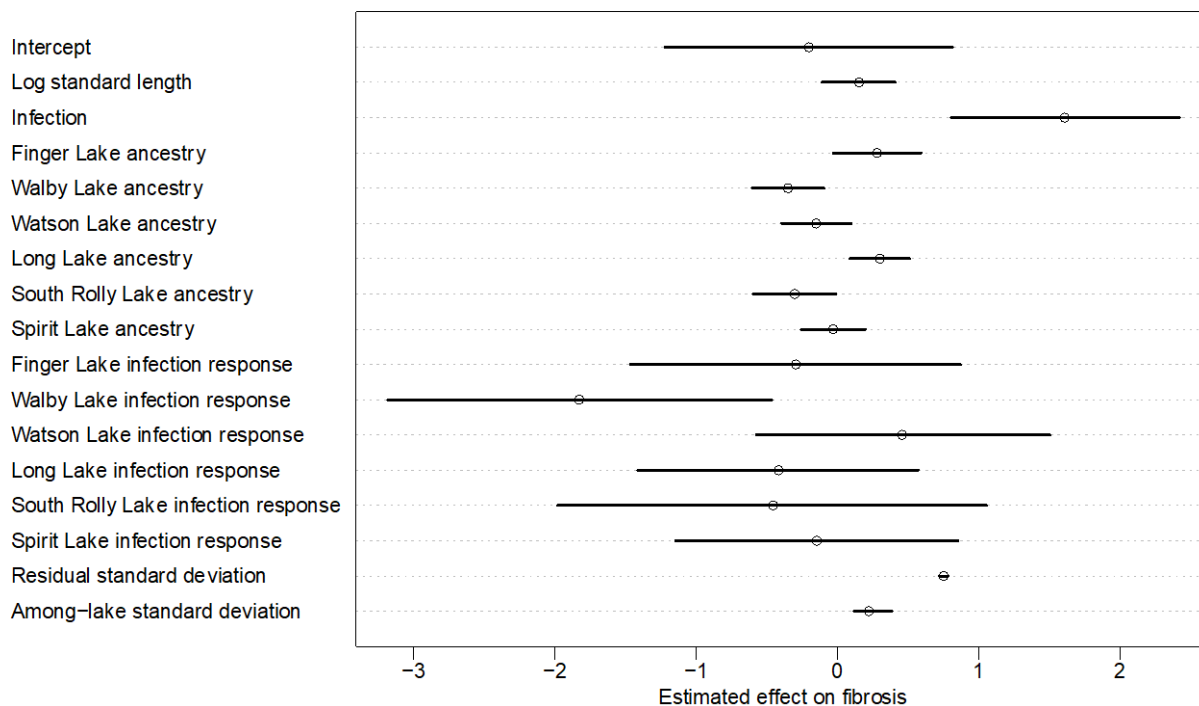
Supplementary figure S4. Alum injection induces fibrosis in all source lake stickleback populations. Lakes are ordered from smallest to largest on the x axis, with an anadromous marine population (Rabbit Slough) on the right to represent the ancestral character state of stickleback before colonizing freshwater (no measured response). For each lake we present the mean fibrosis of control fish (open circles, receiving Phosphate Buffered Saline only), and the mean for the Alum injected fish (1% in PBS) in filled circles. Error bars are 1 standard error. Lakes are color coded by ecomorphology (blue for limnetic, green for benthic). Methods: Injection of an immune adjuvant (alum) induces fibrosis in all stickleback genotypes, though to varying severity (Hund et al. 2022). Two-year-old fish were injected intraperitoneally with either PBS (0.9x endotoxin free PBS) or alum (1% AlumVax Phosphate, OZ Bioscience AP0050), following (Hund et al. 2022). Sample sizes are listed in supplementary table S5. Fish were anesthetized in MS-222 (50 mg/mL, pH 7.4), and injections were administered into the left sider of the peritoneal cavity. Injections were approved by the University of Massachusetts Lowell Institutional Animal Care and Use Committee protocol 21-10-07-Ste. Fish were euthanized in MS-222 (500mg/ml, pH 7.4) 35 days after injection, then dissected to score fibrosis.



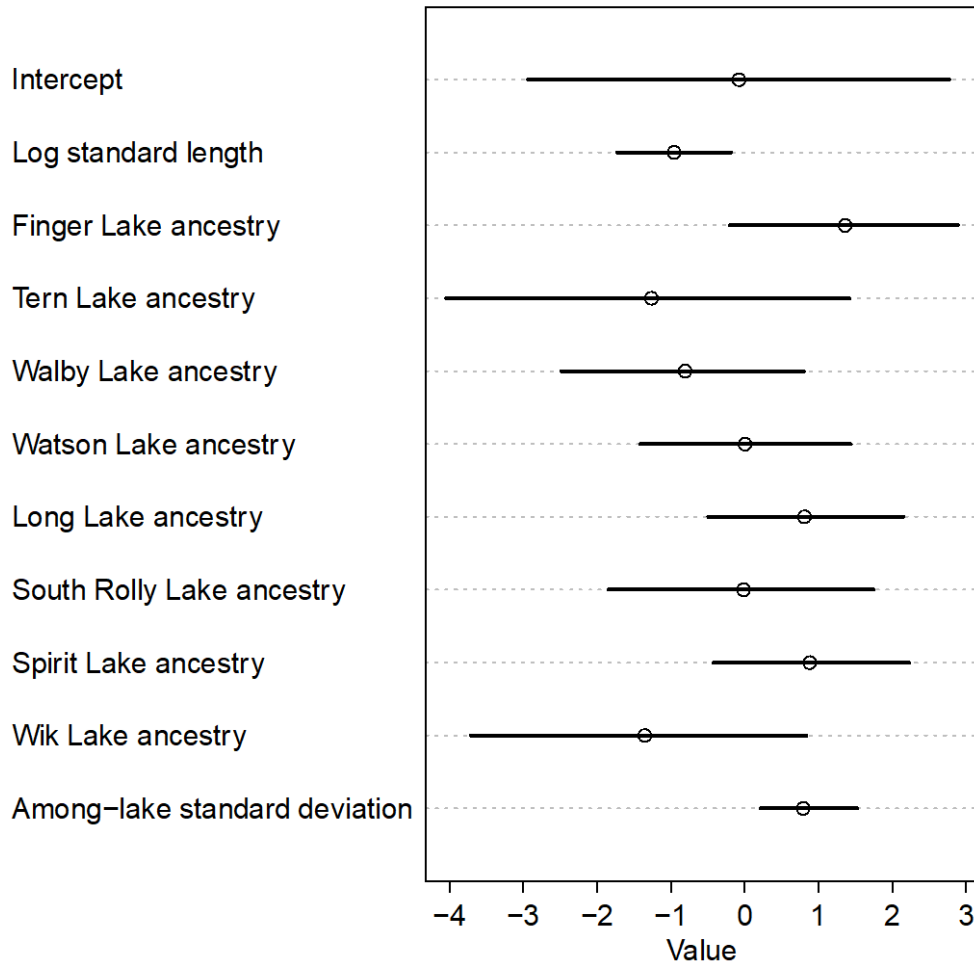
Supplementary figure S5. The correlation between cestode prevalence and mean fibrosis declined from positive to negative from 2020-2025 in the recipient lakes ($r = -0.9354$, $P = 0.0031$). This figure visualizes the changing slopes of regressions shown in fig 5A. Comparisons among recipient lakes show that in 2020-2022 there is a positive relationship between lake-level *S. solidus* prevalence, and mean fibrosis intensity. In 2023 this trend relaxes and in 2024 and 2025 the relationship is negative. Here, we plot the correlation coefficients for each annual line in fig. 5A, as a function of time, to illustrate this temporal change. This is, we should emphasize, a post-hoc analysis motivated by noticing the trend in fig. 5A.



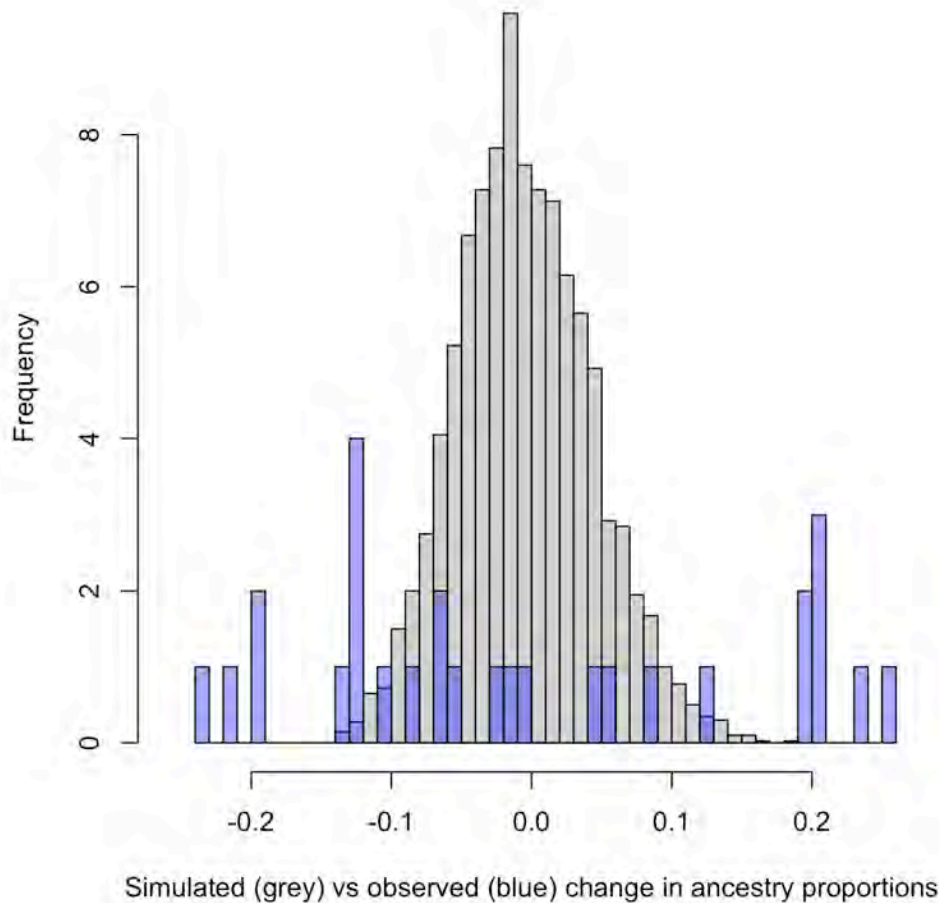
Supplementary figure S6. Tapeworm prevalence exhibits a negative auto-correlation in the source lakes, consistent with fig. 5C. Each point is a particular lake and inter-year period (blue points for 2021-22; turquoise for 2022-23; purple for 23-24). Regression lines are shown for three inter-year periods, solid lines are statistically significant trends ($P < 0.05$). The shaded grey area are disallowed combinations of values (e.g., a parasite with prevalence 0.01 cannot decline by more than 0.01).



Supplementary figure S7. Variation in genotypic responses to infection within recipient lakes. We used a Bayesian linear model to estimate effects of infection, ancestry proportions, and their interactions on within-lake variation in fibrosis, treating recipient lake as a random effect. Here we plot posterior distribution sample means with 95% credibility intervals. Consistent with results reported above (e.g., fig. 2B, Supplement A), there is a positive effect of infection on fibrosis. Baseline fibrosis differs among ancestries. This can reflect genotype-specific responses to prior cestode exposures that failed to generate a detectable infection (e.g., if the fibrosis response successfully eliminated the parasite), because fibrosis persists for many months after a parasite encounter. Thus, the baseline ancestry effects do not entirely represent a parasite-free control. Nevertheless, we detect strong support for additional variation in fibrosis generated by genotype \times infection interactions (ancestry infection responses). WAIC comparisons favor models with some of the genotype \times infection interactions (85% WAIC weight), over models omitting all genotype-specific responses (15% WAIC weight).



Supplementary figure S8. Genetic variation in infection rates within recipient lakes. The figure presents posterior probability means (points) and 95% credible intervals from Bayesian hierarchical linear model analyses of the effect of source lake ancestry, and recipient lake, on *S. solidus* infection probabilities. Effect size estimates indicate which populations contribute increased (positive) or decreased (negative) risk of infection or severe fibrosis. Effect sizes for infection mostly span zero, though there is a clearly positive and non-zero estimate for the among-lake random effect variance.



Supplementary figure S9. Comparison of observed ancestry frequency changes against neutral and sampling null expectations. Ancestry frequencies changed between recipient lake introductions in 2019, and resampling to genotype in 2021 (examples in fig. 6A&B). Here, we evaluate whether the observed changes in genotype frequencies could plausibly be a result of founder effects, genetic drift, and other stochastic sampling processes. To generate the stochastic null expectation we simulated the process by which the genetic data were generated (see R script for supplemental figures in the archive, for details). Briefly, we consider a population founded with 400 fish drawn at random from a large mixed pool of four populations in equal proportions (ancestries A, B, C, and D each were at 25% in the pool). Using the R function *rmultinom* we drew 400 individuals to found a lake population, calculating new ancestry frequencies of the introduced subsample of individuals. We allowed rapid population growth of 50 offspring per fish, using multinomial sampling again to generate F1 ancestry frequencies with genetic drift. A second round of population growth and genetic drift yielded F2 ancestry frequencies. We then used multinomial sampling one more time to simulate drawing 100 individuals to genotype from the F2 population. We calculated the difference between the founding frequencies and F2 sample frequencies, resulting from this purely stochastic process of founder effects, drift, and sampling. We repeated this 1000 times to generate a null distribution for the magnitude of ancestry proportion change expected from null processes. We then calculated the empirically observed ancestry proportion changes in the recipient lakes that received a single pool (e.g., omitting Loon Lake where initial frequencies were

12.5%), which are plotted as blue overlays on the null histogram. This clearly conveys that in the first two generations of breeding in the recipient lakes we observed large changes in ancestry frequencies that are in many cases greater than stochastic sampling processes alone can account for. From this observation we infer that natural selection played a role in driving these large genotype frequency shifts. Note that this test is conservative because our simulations assumed the smallest founder population size (400) whereas most populations were founded with 800 or even 1600 founders, which would result in a narrower null distribution.

Table S1. Experimental design showing the numbers of fish transplanted from source to recipient lakes. Source lakes and recipient lakes are color coded by whether each is considered benthic (green) or limnetic (blue). The initial introduction to G Lake failed for unknown reasons, so we repeated the introduction in 2022 and in 2023 confirmed successful establishment, and reintroduced stickleback into G Lake, equally drawn from all source lakes (except Long, where a pike invasion has caused stickleback collapse). Because the second successful G lake population is not chronologically aligned with other lakes, we do not consider G Lake further in this paper.

		TO RECIPIENT LAKE:									
		G Lake	Leisure Lake	CC Lake	Leisure Pond	Hope Lake	Crystal Lake	Ranchero Lake	Fred Lake	Loon Lake	
FROM SOURCE LAKE:	Benthic	Finger Lake	445	400	202	103					299
		Tern Lake	302	278	191	102					170
		Watson Lake	452	406	202	105					294
		Walby Lake	449	419	202	102					301
	Limnetic	Long Lake					455	400	203	104	287
		South Rolly Lake					444	400	203	109	275
		Spirit Lake					461	400	202	103	300
		Wik Lake					294	294	198	103	172
			1648	1503	797	412	1654	1494	806	419	2098
											10831

Table S2. Sample sizes of source and recipient lakes through years for fibrosis and infection data. Source Lakes were not sampled in 2020 due to COVID. Recipient lake populations were extinct at the time of sampling in 2019, so were not sampled.

		2019	2020	2021	2022	2023	2024	2025	Totals:
Recipient									
Lakes	CC Lake	NA	40	100	50	100	100	100	490
	Crystal Lake	NA	40	100	100	100	100	100	540
	Fred Lake	NA	40	100	50	100	100	100	490
	G Lake *	NA	1	0	0	150	100	100	351
	Hope Lake	NA	40	100	50	100	100	100	490
	Leisure Lake	NA	40	100	100	100	100	100	540
	Leisure Pond	NA	40	100	100	52	0	94	386
	Loon Lake	NA	40	100	81	100	100	100	521
	Ranchero Lake	NA	40	100	50	100	100	100	490
Source									
Lakes	Finger Lake	100	0	30	30	100	100	NA	360
	Jean Lake **	97	NA	NA	NA	NA	NA	NA	97
	Long Lake ***	80	0	30	0	0	0	NA	120
	South Rolly Lake	98	0	30	50	100	60	NA	338
	Spirit Lake	98	0	100	30	100	100	NA	428
	Tern Lake	65	0	30	50	65	100	NA	310
	Walby Lake	100	0	30	30	98	100	NA	358
	Watson Lake	98	0	30	50	100	100	NA	378
	Wik Lake	98	0	100	30	77	55	NA	360
Totals:		834	321	1180	851	1542	1515	894	7,047

* The G Lake introduction failed in 2019-2020 and zero individuals were captured or observed despite intensive checking in 2021. A new reintroduction was attempted in 2022 and succeeded. This paper omits G lake from consideration because we lack multiple years of time series data from it.

** Jean Lake was removed from consideration as a source lake after sampling in 2019.

*** Long Lake stickleback are presumed extinct after pike appeared in 2021 and stickleback catch rates dropped to zero in 2022 and 2023, and was not sampled again.

Table S3: Ancestry genotyping methods are provided here, and the table provides a list of the SNPs unique to each source population that were used to infer ancestry of fish from the recipient lakes. The population abbreviations for each lake are: LG (Long), SL (Spirit), SR (South Rolly), WK (Wik), FG (Finger), TL (Tern), WB (Walby), WT (Watson). Methods: For each source population, we pooled equimolar amounts of DNA from 100 individuals (2019 sample) and used PoolSeq to characterize genomic allele frequencies. Using these published data (Weber et al. 2022), we selected 24 SNPs per source population that were unique to that population. We selected SNPs to maximize the frequency of the unique alleles in the respective source populations, while filtering out SNPs with low read numbers (more than 1.5 SDs fewer than the mean read number) and avoiding effects of linkage by ensuring that every chromosome (excluding the sex chromosome) had at least one SNP. We designed two Fluidigm SNPtype assays, one with SNPs from the benthic source populations and one with SNPs from the limnetic source populations. To validate the efficacy of these assays in correctly inferring ancestry, we genotyped 16 individuals from each source population from samples collected in 2018, all of which were assigned to the correct population based on the genotyping results. This trial run also identified SNPs that were unsuccessful or that underperformed (i.e. were present in the trial fish in much lower frequency than expected from the PoolSeq data); these were omitted from subsequent analyses, leaving 20 private-allele SNPs per population on average. The final list of SNPs, 158 in total with an average private-allele frequency of 81%, can be found in this table. To confirm the accuracy of ancestry inferences with this number of SNPs, we simulated analogous scenarios in R with simulated random mating and recombination and independent assortment. In the simulated F1 generation, we have an error rate of 0.005% in 100 simulations, and in the F2, we have an error rate of 6.5%. For the individuals whose ancestry we mis-infer, we still identify the correct set of ancestral populations (but infer the wrong proportions) about half the time, leaving just 3.5% of F2 individuals where we overlook a contribution from one of the ancestral populations.

Assay	Population	Chromosome	Position	Unique Base	Allele Frequency
Limnetic	LG	chrII	15917728	T	0.76
Limnetic	LG	chrIII	823613	A	0.76
Limnetic	LG	chrIII	9359110	A	0.68
Limnetic	LG	chrIV	20067576	A	0.85
Limnetic	LG	chrIV	13299762	T	0.75
Limnetic	LG	chrV	1753768	A	0.66
Limnetic	LG	chrVI	7405819	A	0.64
Limnetic	LG	chrVII	21415801	T	0.69
Limnetic	LG	chrVIII	14289522	T	0.71
Limnetic	LG	chrX	6603858	T	0.68
Limnetic	LG	chrXI	16193369	C	0.91
Limnetic	LG	chrXI	3081566	A	0.80
Limnetic	LG	chrXII	2375936	A	0.72
Limnetic	LG	chrXIII	8095355	T	0.73
Limnetic	LG	chrXIV	2478199	A	0.61

Limnetic	LG	chrXV	14863116	T	0.56
Limnetic	LG	chrXVII	9235480	T	0.61
Limnetic	LG	chrXVIII	5379465	T	0.67
Limnetic	LG	chrXX	3621731	C	0.69
Limnetic	LG	chrXXI	6464598	A	0.58
Limnetic	SL	chrI	6553442	T	0.90
Limnetic	SL	chrII	7692517	T	0.97
Limnetic	SL	chrII	7692967	A	0.96
Limnetic	SL	chrIII	9231340	C	0.93
Limnetic	SL	chrIV	14839069	T	0.95
Limnetic	SL	chrVI	8431323	A	0.95
Limnetic	SL	chrVI	8425114	A	0.94
Limnetic	SL	chrVII	1817761	A	1.00
Limnetic	SL	chrVIII	3643167	A	0.90
Limnetic	SL	chrX	7342470	A	0.78
Limnetic	SL	chrXVI	7290192	T	0.91
Limnetic	SL	chrXI	931319	T	0.98
Limnetic	SL	chrXIII	591253	T	0.90
Limnetic	SL	chrXIV	11492271	T	0.68
Limnetic	SL	chrXV	504571	A	0.80
Limnetic	SL	chrXVI	10929953	A	0.92
Limnetic	SL	chrXVII	7968281	T	0.88
Limnetic	SR	chrI	26934908	C	1.00
Limnetic	SR	chrI	26952877	A	1.00
Limnetic	SR	chrII	13580477	T	0.92
Limnetic	SR	chrIII	11145910	A	0.78
Limnetic	SR	chrIV	32386335	A	0.97
Limnetic	SR	chrIX	19733496	A	0.93
Limnetic	SR	chrV	9747888	A	0.94
Limnetic	SR	chrV	9747863	C	0.94
Limnetic	SR	chrVI	15534687	A	0.79
Limnetic	SR	chrVII	2508228	A	1.00
Limnetic	SR	chrVIII	18169994	A	0.92
Limnetic	SR	chrX	15470216	A	0.84
Limnetic	SR	chrXI	8508229	T	0.96
Limnetic	SR	chrIX	10856659	T	0.93
Limnetic	SR	chrXII	13556549	A	0.95
Limnetic	SR	chrXIII	3295246	A	0.78
Limnetic	SR	chrXIV	6944009	T	0.89
Limnetic	SR	chrXV	6208432	T	0.72
Limnetic	SR	chrXVI	11846433	A	0.84
Limnetic	SR	chrXVII	6014009	T	0.95
Limnetic	SR	chrXVIII	6861019	T	0.77
Limnetic	SR	chrXX	3592900	A	0.99
Limnetic	SR	chrXX	3813198	T	0.99

Limnetic	SR	chrXXI	11294121	T	0.85
Limnetic	WK	chrI	9646224	C	0.88
Limnetic	WK	chrII	1721718	A	0.71
Limnetic	WK	chrIV	29635767	T	0.95
Limnetic	WK	chrIX	11691955	A	0.77
Limnetic	WK	chrV	9684570	A	0.95
Limnetic	WK	chrV	2195413	T	0.88
Limnetic	WK	chrVI	2510463	T	0.82
Limnetic	WK	chrVI	10480595	T	0.80
Limnetic	WK	chrVII	7026346	A	0.88
Limnetic	WK	chrVIII	6263140	T	0.68
Limnetic	WK	chrX	6995177	A	0.75
Limnetic	WK	chrXI	12958240	T	0.65
Limnetic	WK	chrXII	13741528	T	0.61
Limnetic	WK	chrXIII	14435087	C	0.70
Limnetic	WK	chrXIV	6924894	T	0.81
Limnetic	WK	chrXV	1193653	A	0.70
Limnetic	WK	chrXVI	10258483	T	1.00
Limnetic	WK	chrXVII	7254362	T	0.89
Limnetic	WK	chrXVII	7010766	A	0.87
Limnetic	WK	chrXVIII	14389316	T	0.71
Limnetic	WK	chrXX	13672198	T	0.98
Limnetic	WK	chrXX	13069503	A	0.93
Limnetic	WK	chrXXI	2104869	C	0.65
Benthic	FG	chrI	15704205	T	0.66
Benthic	FG	chrII	8998980	T	0.78
Benthic	FG	chrII	2892706	C	0.76
Benthic	FG	chrIII	11904068	C	0.74
Benthic	FG	chrIV	31662263	T	0.65
Benthic	FG	chrIX	2916678	T	0.74
Benthic	FG	chrV	8194471	C	0.77
Benthic	FG	chrVI	9113425	T	0.61
Benthic	FG	chrVII	20096576	A	0.62
Benthic	FG	chrVIII	7909323	T	0.49
Benthic	FG	chrX	13397132	A	0.58
Benthic	FG	chrXII	2312380	A	0.58
Benthic	FG	chrXIII	3776929	A	0.53
Benthic	FG	chrXIV	13767296	T	0.66
Benthic	FG	chrXV	12722008	A	0.93
Benthic	FG	chrXV	13373000	A	0.80
Benthic	FG	chrXVI	16659604	C	0.70
Benthic	FG	chrXVII	9976657	A	0.69
Benthic	FG	chrXVIII	6306103	A	0.85
Benthic	FG	chrXVIII	14565840	A	0.78
Benthic	FG	chrXX	19635221	A	0.86

Benthic	FG	chrXX	5821398	A	0.76
Benthic	FG	chrXXI	10304559	A	0.49
Benthic	TL	chrI	20114340	C	1.00
Benthic	TL	chrI	20163367	A	1.00
Benthic	TL	chrII	21053847	T	1.00
Benthic	TL	chrIV	5729611	T	1.00
Benthic	TL	chrII	20097809	A	1.00
Benthic	TL	chrIX	348981	C	1.00
Benthic	TL	chrV	2590697	T	1.00
Benthic	TL	chrVI	8817301	C	1.00
Benthic	TL	chrVII	1723789	A	1.00
Benthic	TL	chrX	3733989	T	0.98
Benthic	TL	chrXI	658255	T	0.99
Benthic	TL	chrXII	136786	A	1.00
Benthic	TL	chrXIII	915897	A	1.00
Benthic	TL	chrXV	10269146	A	0.99
Benthic	TL	chrXVI	5926417	A	1.00
Benthic	TL	chrXVII	8487039	T	1.00
Benthic	TL	chrIII	130727	A	1.00
Benthic	TL	chrXVIII	766384	C	0.99
Benthic	TL	chrXX	14862997	A	1.00
Benthic	TL	chrXXI	11630457	A	0.99
Benthic	WB	chrI	11658546	T	0.68
Benthic	WB	chrIII	6828202	T	0.67
Benthic	WB	chrIX	11571874	A	0.92
Benthic	WB	chrIX	11569307	T	0.91
Benthic	WB	chrV	2233732	T	0.62
Benthic	WB	chrVI	11736089	T	0.69
Benthic	WB	chrVII	7165503	T	0.80
Benthic	WB	chrVIII	5789299	C	0.63
Benthic	WB	chrX	651167	T	0.63
Benthic	WB	chrXI	2032558	A	0.84
Benthic	WB	chrXIII	77338	T	0.64
Benthic	WB	chrXIV	5133486	A	0.61
Benthic	WB	chrXV	10053758	A	0.63
Benthic	WB	chrXVI	11188280	A	0.93
Benthic	WB	chrXVII	4145810	T	0.67
Benthic	WB	chrXVIII	4068044	T	0.91
Benthic	WB	chrXVIII	4078056	T	0.90
Benthic	WB	chrXXI	11305884	T	0.84
Benthic	WT	chrI	6268283	A	0.74
Benthic	WT	chrIII	8273044	A	0.63
Benthic	WT	chrIV	25951865	T	0.74
Benthic	WT	chrIV	13840483	A	0.72
Benthic	WT	chrV	7449895	T	0.68

Benthic	WT	chrVII	27191714	T	0.66
Benthic	WT	chrVIII	3764596	A	0.79
Benthic	WT	chrX	3240678	A	0.82
Benthic	WT	chrX	3233056	A	0.82
Benthic	WT	chrXI	11603955	T	0.73
Benthic	WT	chrXII	9432933	A	0.71
Benthic	WT	chrXIII	7970424	A	0.70
Benthic	WT	chrXX	3577020	A	0.75

Table S4. Sample size for lab-based experimental infection assays. Experiment A and B were conducted at separate times, at different ambient temperature regimes. Experiment A used multiple parasite genotypes, whereas B used only Walby Lake parasites.

Population	Experiment	Sample Size	Parasite strain	Fibrosis assayed X days post exposure
Finger	A	11	Finger	43
Finger	A	13	Tern	42-43
Finger	A	10	Walby	42
Finger	A	5	None (copepod only)	13
South Rolly	A	7	Kjerringøy	44-48
South Rolly	A	8	Tern	43-44
Spirit	A	6	Tern	42-44
Spirit	A	6	Walby	42
Spirit	A	4	None (copepod only)	14
Tern	A	4	Kjerringøy	46-48
Tern	A	9	Tern	43
Tern	A	8	Walby	42-43
Walby	A	10	Kjerringøy	42-48
Walby	A	12	Tern	42-48
Walby	A	12	Walby	42
Walby	A	5	None (copepod only)	15
Watson	A	6	Tern	43
Watson	A	6	Walby	43
Wik	A	4	Kjerringøy	41-43
Wik	A	6	Tern	43
Wik	A	6	Walby	42
Watson	B	16	Walby	30
Finger	B	7	Walby	30

Spirit	B	15	Walby	30
Wik	B	2	Walby	30
Watson	B	16	Walby	30
Finger	B	7	Walby	30

Table S5. Sample size for lab-based immunization experiments

Population	PBS	Alum	NPCGG in Alum
Finger Lake	4	5	5
Long Lake	9	9	10
South Rolly Lake	9	8	8
Spirit Lake	11	10	11
Tern Lake	9	10	7
Walby Lake	11	9	12
Watson Lake	11	8	12
Wik Lake	6	6	9

Supplement A

Analysis of the individual-scale relationship between infection and fibrosis

Previous studies demonstrate that *Schistocephalus* infection induces fibrosis in stickleback. Fibrosis tends to be more severe in laboratory-raised individuals who were experimentally infected with *S. solidus*, compared with uninfected siblings (Weber et al. 2022). Individuals injected with *S. solidus* protein extracts exhibit stronger fibrosis than individuals receiving saline injections in the laboratory (Hund et al 2022; Bolnick et al. 2025). In field-caught individuals with unknown exposure histories, stickleback with tapeworms tend to have stronger fibrosis than those without (De Lisle and Bolnick 2021; Hund et al. 2022). These results were all generated using field-caught or lab-bred stickleback from Vancouver Island. In this supplement, we use our data on wild-caught stickleback from this study to evaluate whether the same relationship holds in Alaskan source and recipient lakes.

Source lakes:

We used a linear model to test whether *S. solidus*-infected individuals tend to have more fibrosis than uninfected individuals within the same lake. The linear model included infection (present/absent), fish population (a random effect), and an infection×population interaction. Sex and fish length were initially included as covariates but dropped for lack of explanatory value (based on AIC).

Within the Alaskan source lakes, individual fish infected by tapeworms on average have 1.98-fold stronger fibrosis than those without (fig. 2B; linear model infection effect $F_{1,2405}=14.9$, $P=0.0001$, lake effect $F_{8,2405}=90.8$, $P<0.0001$). The magnitude of this difference varies among lakes from 1.1 to 8.2-fold (lake×infection interaction $F_{7,2405}=23.8$, $P=0.0003$).

Although this association between infection and fibrosis holds among individual fish within nearly all lakes (fig 2B), it is absent at the among-lake level. Source lakes with higher tapeworm prevalence do not have correspondingly higher mean fibrosis ($r = -0.002$, $P = 0.997$). Multiple ecological and genetic variables can influence both values. For instance, low fibrosis can occur

due to low exposure rates, or a genetic inability to respond to exposure. And, high fibrosis can suppress infection leading to low infection rates, though some tapeworm populations might tolerate this immune response (e.g., there is one lake in British Columbia where *S. solidus* thrives in high fibrosis fish). Also, with only eight lakes our power to detect an among-lake correlation is weak.

The variation in fibrosis among recipient lakes only holds for wild-caught fish, or lab-raised fish exposed to *S. solidus* (fig. 2C). In contrast, stickleback injected with an artificial immune stimulant, Aluminum phosphate (Alum), all developed similar fibrosis regardless of population (fig. S.A.1, injection treatment $F_{1,186}=8.9$, $P=0.0032$, Population effect $F_{7,128}=1.3$, $P=0.24$; Population \times treatment interaction $F_{7,128}=0.83$, $P=0.57$). The fact that the fibrosis response is similar among lakes when challenged with Alum highlights that the population differences described above are indeed in relation to *Schistocephalus* infection.

Recipient lakes:

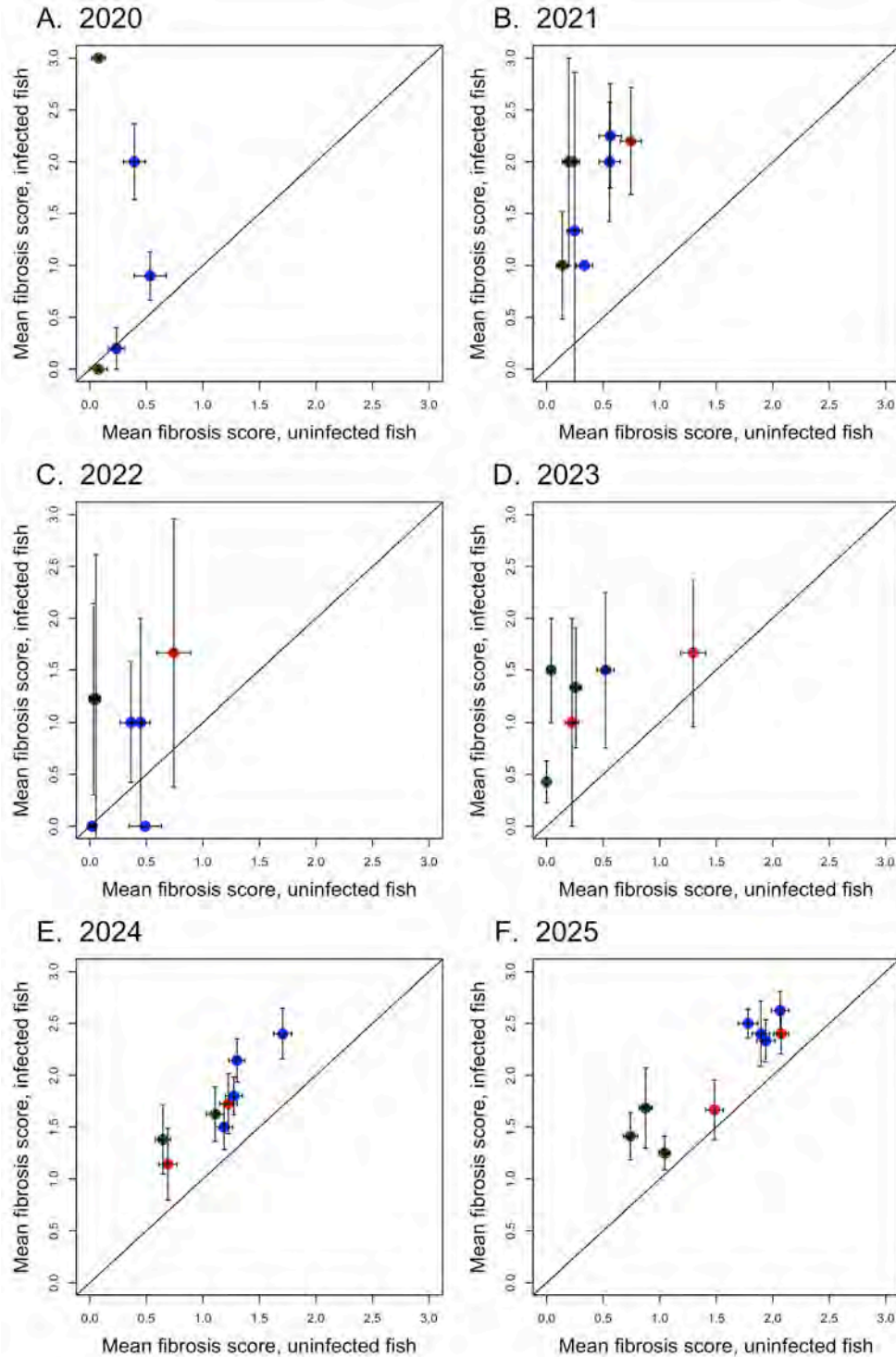
Focusing on the reintroduced populations, we used a linear model to test whether fibrosis of wild-caught individual fish is higher in the presence of a tapeworm infection, with lake and year effects, and all two- and three-way interactions. This replicates an analysis described above for source lake fish. To quantify the fibrosis response to infection, we calculated the log ratio of fibrosis in infected versus uninfected fish, in each lake and year. To test for changing fibrosis responsiveness over time, we regressed these log response ratios against year.

Within the recipient lakes, individual fish with *S. solidus* infection tend to have higher fibrosis than individuals without (ANOVA with effects of lake, year, infection, and their interactions, main effect of infection $F_{1,4109}=249.0$, $P<0.0001$, fig. S.A.2). This result confirms the same pattern seen within source lakes (fig. 2B). We also observe fibrosis variation among lakes ($F_{8,4109}=4275.8$, $P<0.0001$) and among years ($F_{5,4109}=340.4$, $P<0.0001$). There is significant variation in this response among lakes (lake \times infection interaction $F_{8,4109}=2.97$, $P=0.0025$), and among years (year \times infection interaction $F_{5,4109}=$, $P<0.0001$). If fibrosis was a purely plastic response to infection that did not evolve over time, we would not necessarily expect a year \times infection or

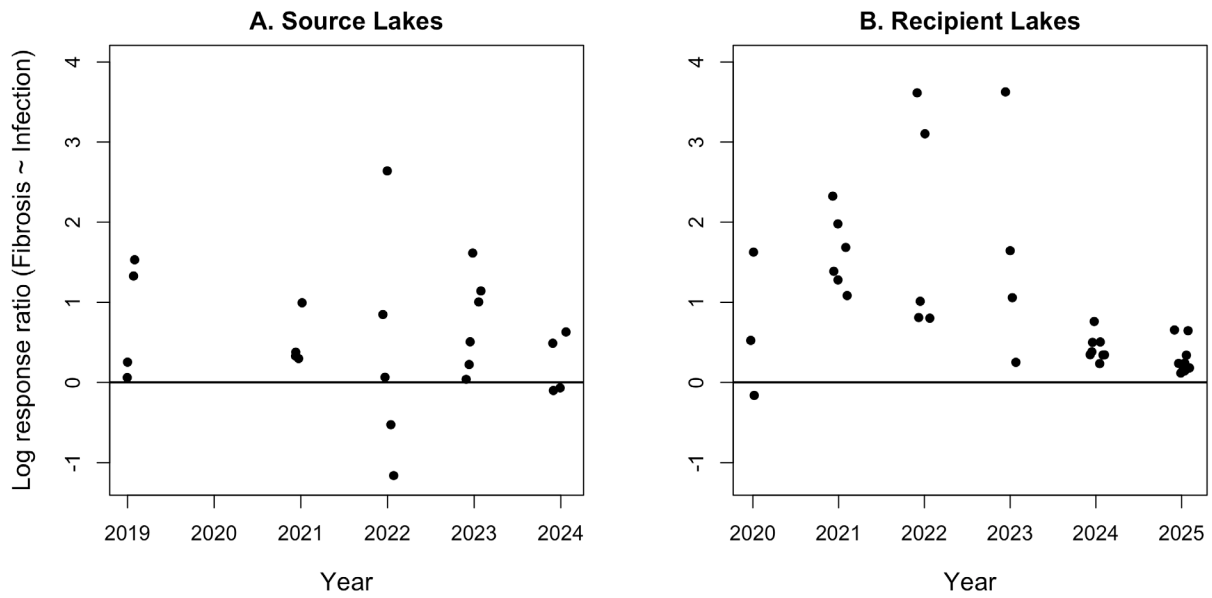
lake×infection interaction effect, both of which are significant. However, there is not a significant lake× year×infection three-way interaction ($F_{30,4109} = 1.10$, $P = 0.335$).

Temporal trends in infection effect on fibrosis

To quantify the strength of the infection-fibrosis association, we calculated a response ratio (logRR). This is the log of the ratio of mean fibrosis in infected / uninfected fish. A log RR of 0 means equal fibrosis, and positive values indicate higher fibrosis in infected than uninfected fish. Figure S.A.3 visualizes temporal trends in fibrosis logRR over years the source and recipient lakes. Two insights emerge from this exercise. First, fibrosis is induced by infection in almost all populations in almost all years. Second, the strength of the infection-fibrosis relationship appears to follow a non-monotonic relationship in the recipient lakes. The logRR increased from 2020 to 2021, then declined thereafter. This decline in response ratio arises because fibrosis increased in both infected and uninfected fish in later years (Fig 4D). The increased fibrosis of uninfected fish may reflect the evolution of constitutively high fibrosis. Or, fish that we classified as uninfected may in fact have been exposed to *S. solidus* prior to our sampling, triggering irreversible fibrosis that eliminated the infection but persisted thereafter.



Supplement Figure S.A.2. In recipient lakes, individual stickleback with cestode infections have higher fibrosis than uninfected individuals from the same lake. Each panel is a successive year. Each point represents a single recipient lake, color coded by the introduced ecotype pool (genotype: green for benthic, blue for limnetic, red for mixed including G lake). One standard error confidence intervals are plotted for estimates of mean fibrosis score for each category of fish. Lakes with no infections in a given year are not plotted.



Supplement figure S.A.3. Variation in the infection-fibrosis relationship (log RR) among lakes, and over time. (A) source and (B) recipient lakes. Note that points are only plotted for lakes with at least 5 tapeworm infections (to allow effective estimates of infection associated fibrosis).

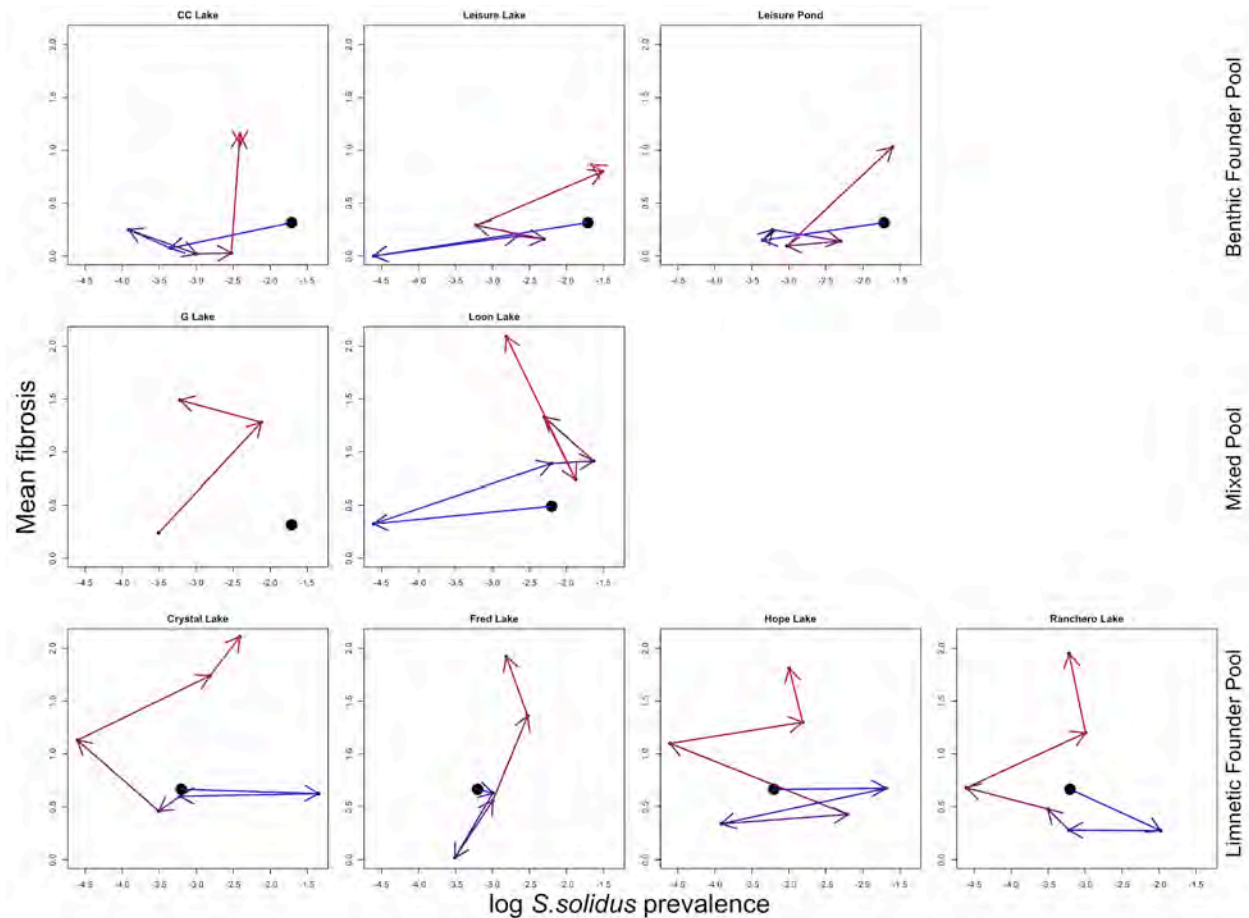
Supplement B

Phase plane visualization of infection-fibrosis dynamics through time.

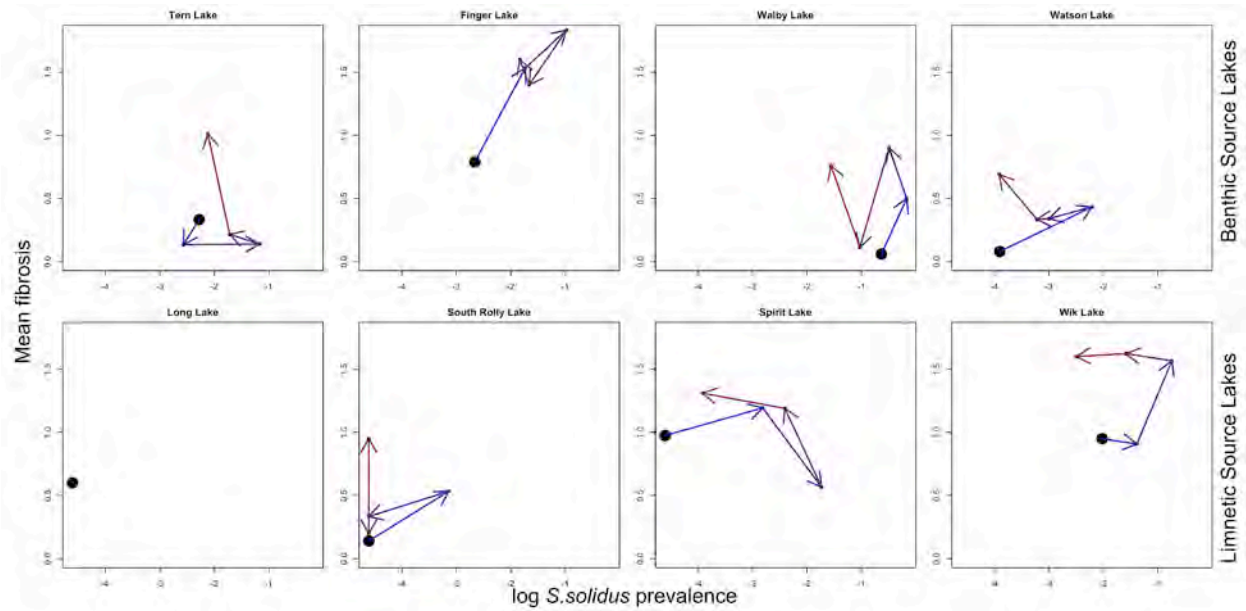
In a recent model of stickleback infection and fibrosis, Sriramulu et al. (2025) examined the consequences of eco-evolutionary dynamics in this system. Numerical simulations generated eco-evolutionary changes that could be plotted on a phase plane with *S. solidus* prevalence (x axis) and fibrosis intensity (y axis). The eco-evolutionary model generated a counter-clockwise loop (fig. S1), in which initially susceptible fish were infected with rare tapeworms, which began to reproduce generating increased infection rates. As infection rate climbed, selection favored alleles with a stronger fibrosis response. The increase in fibrosis then suppressed *S. solidus* prevalence. As tapeworm abundance fell, fewer fish were being stimulated to initiate fibrosis. Ultimately, the parasite was nearly eliminated and fibrosis was scarce. Sriramulu et al (2025) presented empirical data matching this model's prediction, using a 50-year experiment with stickleback added to a quarry pond in British Columbia.

In this supplement, we generate similar phase plane plots using the first half decade of infection and fibrosis changes in the source lakes and recipient lakes. When we plot our recipient lake dynamics on this phase plan (fig. S.B.1), we observe large coupled changes in infection and immunity. However, there is no consistent fit to the predicted counter-clockwise cycle. Indeed some lakes appear to better fit a clockwise trajectory through the phase plane space.

In contrast, the source lakes exhibit smaller between year changes (shorter vectors; fig. S.B.2), consistent with their being closer to equilibrium states. However, the temporal changes within the source lakes often resemble the counter-clockwise cycles from Sriramulu et al's model. Specifically, out of the seven source lakes with enough years of data, six of the populations exhibit consistent counter-clockwise temporal changes fig. S.B.2. This remarkable fit to a previous model (fig. S1) supports our inference that we are seeing eco-evolutionary dynamics even within the relatively stable source lakes.



Supplementary figure S.B.1. A phase plane plot of the joint dynamics of *Schistocephalus solidus* infection prevalence, and fibrosis severity, in the nine recipient lakes (here including G Lake, which we did not otherwise analyze). Each panel is a single lake population, points represent joint values of infection and fibrosis for a given year. Arrows connect values between years starting in 2019 to 2020, then 2020-21, et cetera, ending in 2025. Different colors represent different between-year changes. There are only two arrows for G lake because the initial introduction (solid dot) failed, so after the 2022 reintroduction we have only two between-year transitions from 2023-24, and 2024-25. The top row of lakes received benthic pool founders, and experienced an initial decline in infections and fibrosis, followed by an increase in fibrosis. The middle row are the two lakes receiving mixed pools of founders (G Lake several years after the rest). The bottom row of lakes received limnetic pool founders and all experienced initial increases in infection prevalence. Although the exact temporal trajectory of infection and fibrosis differed between populations, this illustration exhibits the tendency for large changes in fibrosis and infection to coincide, consistent with unstable eco-evolutionary dynamics.



Supplementary figure S.B.2. A phase plane plot of the joint dynamics of *Schistocephalus solidus* infection prevalence, and fibrosis severity, in the eight source lakes. See supplementary fig S7 for details. Here, the top row are benthic source lakes, and the bottom row are limnetic source lakes, as defined by fish ecomorphology. For comparison with fig S.A.1 we keep the axis scales the same, to illustrate that the temporal dynamics in the source lakes are of smaller magnitude. The populations showing the clearest counter-clockwise trajectories consistent with the model include Tern Lake, Watson Lake, and Wik Lake. Walby and Spirit Lakes also generally fit the expected trend.